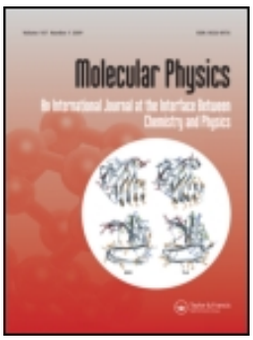

Taylor & Francis
Taylor & Francis Group

Molecular Physics

An International Journal at the Interface Between Chemistry and Physics

ISSN: 0026-8976 (Print) 1362-3028 (Online) Journal homepage: http://www.tandfonline.com/loi/tmph20

Rotation–vibration motion of pyramidal XY_3 molecules described in the Eckart frame: Theory and application to NH_3

Sergei N. Yurchenko , Miguel Carvajal , Per Jensen , Hai Lin , Jingjing Zheng & Walter Thiel

To cite this article: Sergei N. Yurchenko , Miguel Carvajal , Per Jensen , Hai Lin , Jingjing Zheng & Walter Thiel (2005) Rotation–vibration motion of pyramidal XY_3 molecules described in the Eckart frame: Theory and application to NH_3 , Molecular Physics, 103:2-3, 359-378, DOI: 10.1080/00268970512331517255

To link to this article: https://doi.org/10.1080/00268970512331517255

Published online: 21 Feb 2007.

Molecular Physics, Vol. 103, No. 2–3, 20 January–10 February 2005, 359–378

Taylor & Francis
Taylor & Francis Group

Rotation–vibration motion of pyramidal XY_3 molecules described in the Eckart frame: Theory and application to NH_3

SERGEI N. YURCHENKO[†‖], MIGUEL CARVAJAL[‡], PER JENSEN[§*], HAI LIN[¶⊥], JINGJING ZHENG[¶] and WALTER THIEL[¶*]

[†]Steacie Institute for Molecular Sciences, National Research Council of Canada, Ottawa, Ontario, Canada K1A 0R6

[‡]Departamento de Fisica Aplicada, Facultad de Ciencias Experimentales, Avda. de las FF.AA. s/n, Universidad de Huelva, 21071, Huelva, Spain

[§]FB C-Theoretische Chemie, Bergische Universität, D–42097 Wuppertal, Germany

[¶]Max-Planck-Institut für Kohlenforschung, Kaiser-Wilhelm-Platz 1, D–45470 Mülheim an der Ruhr, Germany

(*Received 7 June 2004; in final form 31 July 2004*)

We present a new model for the rotation-vibration motion of pyramidal XY_3 molecules, based on the Hougen–Bunker–Johns approach. Inversion is treated as a large-amplitude motion, while the small-amplitude vibrations are described by linearized stretching and bending coordinates. The rotation–vibration Schrödinger equation is solved variationally. We report three applications of the model to $^{14}NH_3$ using an analytic potential function derived from high-level *ab initio* calculations. These applications address the $J = 0$ vibrational energies up to 6100 cm, the $J \leqslant 2$ energies for the vibrational ground state and the ν_2, ν_4, and $2\nu_2$ excited vibrational states, and the $J \leqslant 7$ energies for the $4\nu_2^+$ vibrational state. We demonstrate that also for four-atomic molecules, theoretical calculations of rotation–vibration energies can be helpful in the interpretation and assignment of experimental, high-resolution rotation–vibration spectra. Our approach incorporates an optimum inherent separation of different types of nuclear motion and thus remains applicable for rotation–vibration states with higher J values where alternative variational treatments are no longer feasible.

1. Introduction

In a recent publication [1] we have reported high-level *ab initio* potential energy surfaces for the NH_3 electronic ground state together with variational calculations of the associated vibrational energies. The corresponding nuclear-motion computer program has also been employed to compute vibrational energies of PH_3 [2]. We have now made some technical improvements of the model used in [1, 2] and extended the theoretical treatment to include rotation. The main purpose of the present paper is to provide a complete description of the nuclear-motion model, which has previously been outlined only very briefly in [1, 2]. We also report calculated vibrational and rotational energies for NH_3 and compare them to experimentally derived term values and to other recent theoretical results [3, 4].

In constructing a quantum mechanical model for the rotation and vibration of a molecule, we are first faced with the problem of choosing suitable coordinates for describing the system. The starting point is a quantum mechanical (or classical) Hamiltonian expressed in terms of the Cartesian coordinates of the nuclei; this Hamiltonian has a simple form but is not very useful for most practical purposes. Generally one has to transform from the Cartesian coordinates to a set of coordinates that facilitate the solution of the rotation–vibration Schrödinger equation. In the present work, we adopt the concept of Hougen, Bunker, and Johns (HBJ) [5] for this coordinate transformation. In the HBJ approach, the molecular coordinates are defined so as to provide maximum separation of the different types of molecular motion: rotation, large-amplitude vibration (i.e. the inversion, 'umbrella-flipping' motion of the NH_3 molecule), and small-amplitude vibration. The extension of the HBJ-formalism to tetra-atomic, ammonia-type molecules was first made by Papoušek *et al.* [6] and

Dedicated to Professor Nicholas C. Handy.

* Corresponding authors. Email: jensen@uni-wuppertal.de (PJ); thiel@mpi-muelheim.mpg.de (WT)

‖ Present address: Max-Planck-Institut für Kohlenforschung, Kaiser-Wilhelm-Platz 1, D-45470 Mülheim an der Ruhr, Germany.

⊥ Present address: Department of Chemistry, University of Minnesota, 334 Smith Hall, 207 Pleasent St. SE. Minneapolis, MN 55455, USA.

Molecular Physics
ISSN 0026–8976 print/ISSN 1362–3028 online © 2005
Taylor & Francis Group Ltd
http://www.tandf.co.uk/journals
DOI: 10.1080/00268970512331517255

culminated in the *nonrigid invertor model* by Špirko [7], in which the rotation–vibration Schrödinger equation is solved by means of perturbation theory.

The basic idea of HBJ is to introduce a flexible *reference configuration* replacing the rigid equilibrium structure of customary rotation–vibration theory (see, for example, [8]). The reference configuration follows the large-amplitude vibration (which, for NH_3, is the inversion) and the remaining small-amplitude vibrations are described as displacements from it. One important aim of our work is to treat highly excited rotational states, and to calculate the energies and wavefunctions of these states accurately we require a model that provides a large degree of separation between rotation and vibration. The HBJ approach is ideally suited in this respect. However, its implementation requires a truncated power series expansion of the rotation–vibration kinetic energy operator in the small-amplitude vibrational coordinates. This approximation can be avoided by expressing the kinetic energy operator entirely in terms of geometrically defined, internal coordinates (typically bond lengths, bond angles, and dihedral angles). With these coordinates, it is possible to derive a kinetic energy operator that is exact within the Born-Oppenheimer approximation. In this latter approach, no measures are taken to minimize rotation–vibration coupling, and therefore the accurate variational calculation of highly excited rotational energies requires an extreme computational effort.

The HBJ approach has been successfully applied to triatomic molecules in the form of the *nonrigid bender model* [9–11] (which is analogous to the nonrigid invertor model in that the Schrödinger equation is solved by perturbation methods) and, more recently, in the form of the MORBID approach [12] which is purely variational. For XH_2 molecules with a relatively heavy central atom, the MORBID treatment has proved to be an efficient tool for studying local mode effects, in particular the formation of near-degenerate clusters of rotation–vibration energies at high rotational excitation [13], and we aim at investigating analogous phenomena in XH_3 molecules. The present theoretical approach for XY_3 molecules has considerable similarity with the MORBID approach for XY_2 molecules, but the two methods differ in one important aspect: Whereas MORBID describes the small-amplitude vibrations by geometrically defined, internal coordinates (e.g. the two bond lengths of a triatomic molecule), the present approach employs *linearized coordinates* (i.e. selected linear combinations of Cartesian displacement coordinates) for this purpose.

During the last decade, *ab initio* electronic-structure methods have come to play an increasingly important role in the theoretical description of molecular rovibronic spectra. Variational calculations on *ab initio* potential energy surfaces now provide rovibronic energies with accuracies comparable to, and sometimes better than, the accuracy obtained in the traditional spectroscopic approach of refining the parameter values of a parameterized, analytical representation of the potential energy surface in least-squares fittings to experimental data. This development is exemplified by recent work on the water molecule (see [14, 15] and the references therein). For the electronic ground state of NH_3, several highly accurate six-dimensional potential energy surfaces have been computed recently [1, 4, 16–18] and variational calculations have been performed on these and other surfaces to describe the vibrational motion in NH_3 [1, 3, 4, 16–27].

The recent work by Colwell *et al.* [3] is similar to ours in that it introduces a variational treatment of rotation *and* vibration for NH_3, considering all vibrational modes explicitly. Their theoretical approach differs from ours in that it employs a kinetic energy operator expressed entirely in terms of geometrically defined, internal coordinates; this operator is exact within the Born-Oppenheimer approximation. We compare our results to the reported [3] theoretical $J = 0, 1, 2$ energies for low-lying vibrational states. In addition, we calculate the rotational structure in the $4\nu_2^+$ vibrational state[1] of NH_3 up to $J=7$, which allows us to make a critical evaluation of the tentative assignments of 55 weak transitions to the lower inversion component of the $4\nu_2$ state of NH_3; these transitions were observed in a recent experimental study of the ν_1, ν_3, and $2\nu_4$ bands [28].

The article is structured as follows. In section 2 we discuss the symmetry properties of pyramidal XY_3 molecules. In section 3 we construct the coordinate transformation to the non-rigid reference coordinate system and introduce the linearized coordinates. In section 4 we derive the kinetic energy operator and pseudo-potential function. We introduce the MORBID-type representation for the potential energy surfaces of ammonia in section 5, where the numerical procedure for calculating the expansion coefficients is also discussed. The basis set for the variational calculations is given in section 6. In section 7 we return to the symmetry properties of ammonia concerning the matrix element calculations. In section 8 we discuss technical details of the variational calculations, such as computation of the Hamiltonian matrix elements, size of the basis set, and convergence. Finally, in section 9 we apply

[1]The superscript + indicates the lower (symmetric) inversion component; the upper (antisymmetric) component is indicated by a superscript –.

the developed theory to NH_3: We calculate vibrational energies to high excitation as well as low-J rotational energies in selected vibrational states, and as mentioned above, we investigate the energies of the states involved in experimentally observed [28] transitions to the $4\nu_2^+$ vibrational state.

2. Coordinates and symmetry

The potential energy surface for the electronic ground state of NH_3 has two different, equivalent minima separated by a relatively small energy barrier of approximately $1800\,cm^{-1}$ [1, 17, 24, 26, 29, 30]. The tunneling through the barrier by 'umbrella-flipping' inversion motion takes place on the time scale of a typical spectroscopic experiment so that the resulting energy splittings ($0.79\,cm^{-1}$ for the rovibrational ground state [7]) are easily observable. Consequently, the appropriate molecular symmetry (MS) group [31] is $\mathcal{D}_{3h}(M)$. The two equilibrium structures are mirror images of each other; we can call them the 'clockwise structure' and the 'anti-clockwise structure'. The protons are labeled 1, 2, 3, and in the clockwise (anti-clockwise) structure a rotation from proton 1 to proton 2 and on to proton 3 is a clockwise (an anti-clockwise) rotation for an observer sitting on the nitrogen nucleus (labeled as nucleus 4). For phosphine PH_3, the inversion barrier is so high (about $12000\,cm^{-1}$ [32]) that no tunneling takes place on the time scale of a typical spectroscopic experiment, and hence the appropriate MS group is $\mathcal{C}_{3v}(M)$ [31].

To describe the symmetries in $\mathcal{D}_{3h}(M)$ of the vibrational and rotational coordinates for NH_3, we use the same conventions for the permutation–inversion operations as in section 15.4.1 of [31]. Our choice of the vibrational coordinates is based on geometrically defined coordinates, i.e. on the bond lengths and interbond angles. The instantaneous internuclear distance N–H_i ($i = 1, 2, 3$) between the N nucleus and proton i is denoted r_i. The bond lengths r_i along with corresponding Morse-type variables are used to characterize the stretching motion in the molecule. The interbond angle α_{ij} is defined as the angle between the N–H_i and N–H_j bonds. We introduce symmetrized combinations of the bond angles below (section 3).

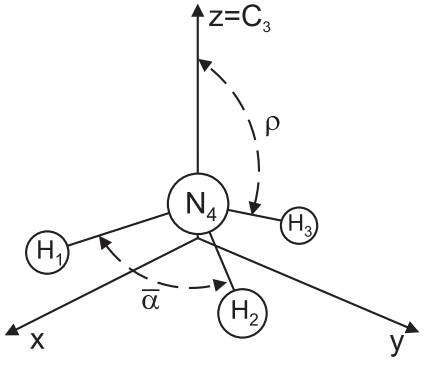

Figure 1. Reference configuration and numbering chosen for ammonia. The origin of the molecule fixed axis system coincides with the centre of mass.

The reference configuration is defined as having all three N–H bond lengths equal to their equilibrium values and all three H–N–H angles equal [6], and it thus has $\mathcal{C}_{3v}$ symmetry. A right handed molecule fixed axis system xyz is attached to the reference configuration of the molecule. The origin is at the centre of mass. The C_3 axis z is directed so that on rotating from H_1 to H_2 to H_3 a right handed screw is driven along the positive z direction (see figure 1). The x axis is chosen so that the xz plane contains the nitrogen nucleus and the proton H_1 with the x coordinate of H_1 being positive. Rotation is described in terms of conventional Euler angles θ, ϕ, χ that define the orientation of the xyz axis system in space; see figure 10–1 of [31].

Following HBJ [5] and Papoušek *et al.* [6], we introduce an inversion coordinate ρ to describe the 'umbrella-flipping' motion. It is defined in terms of the Eckart and Sayvetz conditions [31], see equations (8–10) in section 3. In the mathematical treatment, the coordinate ρ formally plays the role of a fourth rotational angle; the Hamiltonian depends on it in a manner analogous to the way that it depends on the three conventional Euler angles θ, ϕ, χ [5]. The angle ρ has no straightforward geometrical interpretation. Only when the molecule is in the reference configuration is ρ the angle between the symmetry axis C_3 and any one of the bonds (see figure 1).

Table 1 gives the irreducible representations of $\mathcal{D}_{3h}(M)$. The symmetry transformations of the vibrational coordinates, the Euler angles, the components of total angular momentum **J** in the molecular fixed axis system, and the inversion conjugate momentum $J_\rho = -i\hbar\partial/\partial\rho$ are given in table 2. From the characters in table 1 we deduce that the irreducible representations of the stretching coordinates are A_1' and E'. The two bending coordinates transform according to the E' irreducible representation and the inversion coordinate ρ has the symmetry A_2''. In table 1 and 2, we show only one symmetry operation for each group class.

3. Coordinate transformations

To derive the quantum kinetic energy operator we perform a coordinate transformation in the classical

Table 1. The character table of the $\mathcal{D}_{3h}(M)$ group [31].

Γ	E	(123)	(23)	E^*	(123)*	(23)*	
A_1'	1	1	1	1	1	1	$\frac{1}{\sqrt{3}}(r_1+r_2+r_3)$, $\sin\rho$
A_1''	1	1	1	−1	−1	−1	
A_2'	1	1	−1	1	1	−1	J_z
A_2''	1	1	−1	−1	−1	1	$\cos\rho$, J_ρ
E'	2	−1	0	2	−1	0	$\left\{\frac{1}{\sqrt{6}}(2\alpha_{23}-\alpha_{13}-\alpha_{12}), \frac{1}{\sqrt{2}}(\alpha_{13}-\alpha_{12})\right\}$
E''	2	−1	0	−2	1	0	$\{J_x, J_y\}$

Table 2. Transformation of the internal coordinates, the Euler angles and the components of the molecule fixed angular momentum and the inversion conjugate momentum by the symmetry operations of the permutation–inversion group $\mathcal{D}_{3h}(M)$.

Variables	$\{E\}$	$\{(23)\}$	$\{(123)\}$	$\{E^*\}$	$\{(23)^*\}$	$\{(123)^*\}$
r_1	r_1	r_1	r_3	r_1	r_1	r_3
r_2	r_2	r_3	r_1	r_2	r_3	r_1
r_3	r_3	r_2	r_2	r_3	r_2	r_2
α_{23}	α_{23}	α_{23}	α_{12}	α_{23}	α_{23}	α_{12}
α_{13}	α_{13}	α_{12}	α_{23}	α_{13}	α_{12}	α_{23}
α_{12}	α_{12}	α_{13}	α_{13}	α_{12}	α_{13}	α_{13}
ρ	ρ	$\pi-\rho$	ρ	$\pi-\rho$	ρ	$\pi-\rho$
θ	θ	$\pi-\theta$	θ	θ	$\pi-\theta$	θ
ϕ	ϕ	$\phi+\pi$	ϕ	ϕ	$\phi+\pi$	ϕ
χ	χ	$2\pi-\chi$	$\chi-2\pi/3$	$\chi+\pi$	$\pi-\chi$	$\chi+\pi/3$
J_x	J_x	J_x	$-\frac{1}{2}J_x-\frac{\sqrt{3}}{2}J_y$	$-J_x$	$-J_x$	$\frac{1}{2}J_x+\frac{\sqrt{3}}{2}J_y$
J_y	J_y	$-J_y$	$\frac{\sqrt{3}}{2}J_x-\frac{1}{2}J_y$	$-J_y$	J_y	$-\frac{\sqrt{3}}{2}J_x+\frac{1}{2}J_y$
J_z	J_z	$-J_z$	J_z	J_z	$-J_z$	J_z
J_ρ	J_ρ	$-J_\rho$	J_ρ	$-J_\rho$	J_ρ	$-J_\rho$

Hamiltonian, which is then quantized by applying standard procedures [31, 33–35] as explained in section 4. The Cartesian coordinates in the space fixed axis system are transformed to the internal coordinates in the non-rigid reference configuration system [5], where the large-amplitude motions (rotation and inversion) are treated explicitly, while other vibrational modes are considered as small displacements from the reference geometry.

The coordinate transformation between the space fixed axis system XYZ and the molecule fixed axis system xyz is given by [5]:

$$\mathbf{R}_i = \mathbf{R}_{\mathrm{CM}} + S^{-1}(\theta,\phi,\chi)[\mathbf{a}_i(\rho)+\mathbf{d}_i], \tag{1}$$

which is subject to seven constraints (the Eckart [36] and Sayvetz [37] conditions) given as equations (8–10) below. Owing to the constraints, the numbers of independent variables on both sides of the equation become equal. In equation (1) the vector $\mathbf{R}_i$ points to the position of nucleus i, and $\mathbf{R}_{\mathrm{CM}}$ points to the position of the nuclear centre of mass in the space fixed system. A 3×3 orthogonal transformation matrix $S^{-1}(\theta,\phi,\chi)$, expressed in terms of the Euler angles $\{\theta,\phi,\chi\}$ [8], rotates XYZ to xyz; the vector $\mathbf{d}_i$ [with components (d_{ix}, d_{iy}, d_{iz})] gives the displacement, due to small-amplitude vibration, of nucleus i from its reference position $\mathbf{a}_i(\rho)$ in the molecular fixed system. The coordinates of the reference-configuration vectors $\mathbf{a}_i(\rho)$ are defined in [6] for NH_3:

$$a_{1,x} = r_e\sin\rho, \tag{2}$$

$$a_{2,x} = a_{3,x} = -\frac{1}{2}r_e\sin\rho, \tag{3}$$

$$a_{4,x} = a_{1,y} = a_{4,y} = 0, \tag{4}$$

$$a_{2,y} = -a_{3,y} = \frac{\sqrt{3}}{2}r_e\sin\rho, \tag{5}$$

$$a_{1,z} = a_{2,z} = a_{3,z} = \frac{m_{\mathrm{N}}r_e\cos\rho}{3m_{\mathrm{H}}+m_{\mathrm{N}}}, \tag{6}$$

$$a_{4,z} = -\frac{3m_{\mathrm{H}}r_e\cos\rho}{3m_{\mathrm{H}}+m_{\mathrm{N}}}, \tag{7}$$

where m_H and m_N are the nuclear masses of hydrogen and nitrogen, respectively, and r_e is the equilibrium bond length.

In terms of the $\mathbf{a}_i(\rho)$ vectors, the Eckart [36] and Sayvetz [37] conditions are given by:

$$\sum_{i=1}^{N} m_i \, \mathbf{d}_i = 0, \tag{8}$$

$$\sum_{i=1}^{N} m_i \, (\mathbf{a}_i(\rho) \times \mathbf{d}_i) = 0, \tag{9}$$

$$\sum_{i=1}^{N} m_i \, \frac{d\mathbf{a}_i(\rho)}{d\rho} \cdot \mathbf{d}_i = 0, \tag{10}$$

where the sums run over all the nuclei of the molecule and m_i is the mass of the nucleus i. The conditions (8–10) have the following physical meanings: The first Eckart condition in equation (8) keeps the nuclear centre of mass at the origin of the xyz fixed system. The second Eckart condition in equation (9) and the Sayvetz condition in equation (10) reduce the rotation–vibration and the inversion-vibration interactions, respectively [31]. For a given instantaneous nuclear geometry, the values of ρ and the rotational coordinates θ, ϕ, χ can be determined by solving equations (8–10).

We must define five small-amplitude vibrational coordinates in addition to the rotation-inversion coordinates θ, ϕ, χ, and ρ. An obvious choice would be the geometrically defined coordinates r_1, r_2, r_3, combined with suitable linear combinations of the interbond angles α_{12}, α_{23}, and α_{13}, but we have decided to use linearized internal coordinates [38] since they provide a simpler coordinate transformation. The linearized internal coordinates S_n^l are given as linear combinations of the Cartesian displacements as

$$S_n^\ell = \sum_{i=1}^{N} \sum_{\alpha=x,y,z} B_{n,i\alpha}(\rho) \, d_{i\alpha}; \quad n = 1, 2, 3, 4a, 4b, \tag{11}$$

where the subscript α is used to denote the axes (x, y, z), $B_{n,i\alpha}(\rho)$ is an element of a ρ-dependent transformation matrix [39], and N is the number of nuclei. To obtain the matrix elements $B_{n,i\alpha}(\rho)$ we first introduce a set of geometrically defined coordinates $(\Delta r_1, \Delta r_2, \Delta r_3, S_{4a}, S_{4b})$, where Δr_i are bond length displacements from the equilibrium value r_e, and the symmetrized combinations of the instantaneous interbond angles α_{ij} are given by:

$$S_{4a} = \frac{1}{\sqrt{6}}(2\,\alpha_{23} - \alpha_{13} - \alpha_{12}), \tag{12}$$

$$S_{4b} = \frac{1}{\sqrt{2}}(\alpha_{13} - \alpha_{12}). \tag{13}$$

The geometrically defined, internal coordinates S_n $(= \Delta r_1, \Delta r_2, \Delta r_3, S_{4a}$, or $S_{4b})$ can be represented exactly as infinite-order, power-series expansions in the Cartesian displacements $d_{i\alpha}$. When we truncate these power-series expansions after the first order terms and define

$$B_{n,i\alpha}(\rho) = \left(\frac{\partial S_n}{\partial d_{i\alpha}}\right)_{(\mathrm{ref})}, \tag{14}$$

where the derivative is calculated in the reference configuration, we obtain equation (11). The linearized coordinates S_n^ℓ thus coincide with curvilinear ones S_n in the linear approximation $S_n \sim S_n^\ell + O(d_{i\alpha}^2)$. The quantities S_{4a}^ℓ, S_{4b}^ℓ are the first and second components, respectively, of the E' degenerate bending coordinates

$$S_{4a}^\ell = \frac{1}{\sqrt{6}}(2\,\Delta\alpha_{23}^\ell - \Delta\alpha_{13}^\ell - \Delta\alpha_{12}^\ell), \tag{15}$$

$$S_{4b}^\ell = \frac{1}{\sqrt{2}}(\Delta\alpha_{13}^\ell - \Delta\alpha_{12}^\ell). \tag{16}$$

The linearized bond length displacements Δr_k^ℓ and the linearized interbond-angle displacements $\Delta\alpha_{kl}^\ell$ are given by [31]:

$$\Delta r_k^\ell = \sum_{\beta=x,y,z} \frac{a_{k\beta} - a_{4\beta}}{r_e}(d_{k\beta} - d_{4\beta}), \tag{17}$$

$$\Delta\alpha_{kl}^\ell = -\frac{1}{r_e^2 \sin\alpha_e} \sum_{\beta=x,y,z} \times \Big[\big[(a_{l\beta} - a_{4\beta}) - \cos\alpha_e (a_{k\beta} - a_{4\beta})\big](d_{k\beta} - d_{4\beta}) + \big[(a_{k\beta} - a_{4\beta}) - \cos\alpha_e (a_{l\beta} - a_{4\beta})\big](d_{l\beta} - d_{4\beta}) \Big], \tag{18}$$

where r_e and α_e are the equilibrium values of the bond length and the interbond angle, respectively. Equations (17–18) are derived from the first-order expansion in $d_{i\alpha}$

of the following geometrical expressions:

$$r_e + \Delta r_k = \sqrt{\sum_{\beta=x,y,z} \left[(a_{k\beta} - a_{4\beta}) + (d_{k\beta} - d_{4\beta})\right]^2}, \quad (19)$$

$$\cos(\alpha_e + \Delta\alpha_{kl}) = \frac{[(\mathbf{a}_k - \mathbf{a}_4) + (\mathbf{d}_k - \mathbf{d}_4)] \cdot [(\mathbf{a}_l - \mathbf{a}_4) + (\mathbf{d}_l - \mathbf{d}_4)]}{(r_e + \Delta r_k)(r_e + \Delta r_l)}. \quad (20)$$

The nonzero matrix elements $B_{k,i\beta}$ are given by:

$$B_{k,i\beta} = \frac{a_{i\beta} - a_{4\beta}}{r_e}\delta_{k,i} = -B_{k,4\beta}, \quad k = 1,2,3, \quad (21)$$

$$B_{4a,i\beta} = \frac{1}{\sqrt{6}}\left(2\bar{B}_{23,i\beta} - \bar{B}_{13,i\beta} - \bar{B}_{12,i\beta}\right), \quad (22)$$

$$B_{4b,i\beta} = \frac{1}{\sqrt{2}}\left(\bar{B}_{13,i\beta} - \bar{B}_{12,i\beta}\right). \quad (23)$$

where $\beta = x, y, z$ and

$$\bar{B}_{kl,i\beta} = -\frac{1}{r_e^2 \sin\alpha_e}\left[(a_{l\beta} - a_{4\beta}) - \cos\alpha_e(a_{k\beta} - a_{4\beta})\right]\delta_{k,i} - \frac{1}{r_e^2 \sin\alpha_e}\left[(a_{k\beta} - a_{4\beta}) - \cos\alpha_e(a_{l\beta} - a_{4\beta})\right]\delta_{l,i}, \quad (24)$$

$$\bar{B}_{kl,4\beta} = -\bar{B}_{kl,k\beta} - \bar{B}_{kl,l\beta}, \; k,l = 1,2,3 \text{ and } k \neq l. \quad (25)$$

The coordinate transformation inverse to equation (11) can be written as:

$$d_{i\alpha} = \sum_{n=1}^{3N-7} A_{i\alpha,n} S_n^\ell, \quad (26)$$

where the coefficients $A_{i\alpha,n}$ are obtained by solving a system of $3N \times (3N-7)$ linear equations

$$\sum_{i=1}^{N} m_i A_{i\alpha,n} = 0, \quad (27)$$

$$\sum_{i=1}^{N} \sum_{\beta,\gamma=x,y,z} m_i \epsilon_{\alpha\beta\gamma} a_{i\beta} A_{i\gamma,n} = 0, \quad (28)$$

$$\sum_{i=1}^{N} \sum_{\beta=x,y,z} m_i \frac{da_{i\beta}(\rho)}{d\rho} A_{i\beta,n} = 0, \quad (29)$$

$$\sum_{i=1}^{N} \sum_{\beta=x,y,z} B_{m,i\beta} A_{i\beta,n} = \delta_{m,n}, \quad (30)$$

where $\epsilon_{\alpha\beta\gamma}$ is the fully antisymmetric tensor, α assumes the values x, y, or z, and $n, m = 1, 2, 3, \ldots, 3N-7$. Equations (27–29) follow from the Eckart (8,9) and the Sayvetz condition (10), while we obtain equation (30) by inserting equation (26) in equation (11).

The coordinate transformation implemented here [equations (1,26)] is fully determined by the quantities $a_{i\alpha}$ and $A_{i\alpha,n}$. The vector components $a_{i\alpha}$ are defined by equations (2–7), while the matrix elements $A_{i\alpha,n}$ are derived analytically by solving equations (27–30). The matrix elements $a_{i\alpha}$ and $A_{i\alpha,n}$ are simple functions of the inversion coordinate ρ, the masses m_i, and the equilibrium parameter r_e.

Equations (1) and (26) define the transformation between the Cartesian coordinates $(R_{i,X}, R_{i,Y}, R_{i,Z})$ of each nucleus in the space-fixed system and the generalized coordinates contained in the vector

$$\mathbf{q} = (R_X^{\mathrm{CM}}, R_Y^{\mathrm{CM}}, R_Z^{\mathrm{CM}}, \theta, \phi, \chi, \Delta r_1^\ell, \Delta r_2^\ell, \Delta r_3^\ell, S_{4a}^\ell, S_{4b}^\ell, \rho). \quad (31)$$

We use q_λ ($\lambda = 1, \ldots, 12$) to denote a general element of $\mathbf{q}$. The q_λ coordinates define three types of motions: (a) the translational motion described by $(R_X^{\mathrm{CM}}, R_Y^{\mathrm{CM}}, R_Z^{\mathrm{CM}})$ coordinates, (b) the overall rotation described by (θ, ϕ, χ) coordinates, and (c) the relative motions of the nuclei described by the internal coordinates $(\Delta r_1^\ell, \Delta r_2^\ell, \Delta r_3^\ell, S_{4a}^\ell, S_{4b}^\ell, \rho)$. The associated, generalized momenta are given by:

$$\Pi = (P_X, P_Y, P_Z, J_x, J_y, J_z, p_1^\ell, p_2^\ell, p_3^\ell, p_{4a}^\ell, p_{4b}^\ell, J_\rho), \quad (32)$$

where P_F ($F = X, Y, Z$) is the momentum conjugate to the translational coordinate R_F^{CM} (these translational momenta are of no spectroscopic interest in the absence of external fields), (J_x, J_y, J_z) are xyz components of the total angular momentum [8, 31], p_n^ℓ ($n = 1, 2, 3, 4a, 4b$) is the momentum conjugate to the linearized vibrational coordinate S_n^ℓ, and J_ρ is the momentum conjugate to ρ, i.e. quantum mechanically

$$\hat{J}_\rho = -i\hbar\frac{\partial}{\partial\rho}. \quad (33)$$

We use Π_λ ($\lambda = 1, \ldots, 12$) to denote a general element of Π.

The vector $\mathbf{R}_i$ ($i = 1 \ldots N$) in equation (1) has the space fixed coordinates (R_{iX}, R_{iY}, R_{iZ}) and the momentum conjugate to R_{iF}, $F = X, Y, Z$, is denoted P_{iF}. The transformation from generalized momenta Π_λ to

the Cartesian conjugate momenta P_{iF} $(i = 1 \ldots N, F = X, Y, Z)$,

$$P_{iF} = \sum_{\lambda=1}^{3N} s_{\lambda, iF}\, \Pi_\lambda, \tag{34}$$

is defined by a Jacobian matrix with elements

$$s_{\lambda, iF} = \frac{\partial q_\lambda}{\partial R_{iF}}. \tag{35}$$

We assume that the $3N$-dimensional square matrix with elements $s_{\lambda, iF}$ is non-singular so that it can be inverted by means of the chain rule:

$$\sum_{i=1}^{N} \sum_{F=X, Y, Z} \frac{\partial q_\lambda}{\partial R_{iF}} \frac{\partial R_{iF}}{q_\mu} = \delta_{\lambda, \mu}, \tag{36}$$

or

$$\sum_{i=1}^{N} \mathbf{s}_{\lambda, i} \cdot \mathbf{t}_{i, \mu} = \delta_{\lambda, \mu}. \tag{37}$$

We have introduced here the elements $t_{iF, \lambda}$ of the matrix effecting the transformation between Cartesian and generalized classical velocities:

$$\frac{dR_{iF}}{dt} = \sum_{\lambda=1}^{3N} t_{iF, \lambda} \frac{dq_\lambda}{dt} \tag{38}$$

where t is time and

$$t_{iF, \lambda} = \frac{\partial R_{iF}}{\partial q_\lambda}, \tag{39}$$

$i = 1 \ldots N, \quad F = X, Y, Z \quad$ and $\quad \lambda = 1, 2, \ldots, 3N$. Following [33], we establish the correspondence between the XYZ and xyz representations of the vectors $\mathbf{t}_{i, \lambda}$ and $\mathbf{s}_{\lambda, i}$ as

$$\mathbf{s}_{\lambda, i} = \sum_{F=X, Y, Z} \mathbf{e}_F\, s_{\lambda, iF} = \sum_{\alpha=x, y, z} \mathbf{e}_\alpha\, s_{\lambda, i\alpha}, \tag{40}$$

$$\mathbf{t}_{i, \lambda} = \sum_{F=X, Y, Z} \mathbf{e}_F\, t_{iF, \lambda} = \sum_{\alpha=x, y, z} \mathbf{e}_\alpha\, t_{i\alpha, \lambda}, \tag{41}$$

where $\mathbf{e}_F$ and $\mathbf{e}_a$ are the orthogonal, normalized basis vectors. The index α runs over x, y, z, and F runs over X, Y, Z.

The classical rovibrational kinetic energy can be written as [33, 34]:

$$T = \frac{1}{2} \sum_{i=1}^{N} \sum_{F=X, Y, Z} m_i^{-1}\, P_{iF} P_{iF} = \frac{1}{2} \sum_{\lambda=1}^{3N} \sum_{\mu=1}^{3N} \Pi_\lambda\, G_{\lambda, \mu}\, \Pi_\mu, \tag{42}$$

where

$$G_{\lambda, \mu} = \sum_{\alpha=x, y, z} \sum_{i=1}^{N} \frac{s_{\lambda, i\alpha} s_{\mu, i\alpha}}{m_i}. \tag{43}$$

That is, the expression for the classical kinetic energy in terms of the momenta conjugate to the generalized coordinates q_λ is defined by the matrix elements $s_{\lambda, i\alpha}$.

The coefficients $t_{i\alpha, \lambda}$ associated with translation, rotation, inversion and vibration have simple analytical representations [33]:

$$\begin{aligned} t_{iF, F'} &= \delta_{F, F'} \quad \text{translation} \\ t_{i\alpha, \beta} &= \sum_\gamma \epsilon_{\alpha\beta\gamma} R_{i\gamma} \quad \text{rotation} \\ t_{i\alpha, \rho} &= \partial R_{i\alpha} / \partial \rho \quad \text{inversion} \\ t_{i\alpha, n} &= \partial R_{i\alpha} / \partial S_n^\ell \quad \text{vibration.} \end{aligned} \tag{44}$$

It follows from the straightforward coordinate transformation $R_{i\alpha} = R_{i\alpha}(\mathbf{q})$ in equation (1) that the matrix elements $t_{i\alpha, \mu}$ are simple analytical functions of the generalized coordinates $\mathbf{q} : t_{i\alpha, \mu} = t_{i\alpha, \mu}(\mathbf{q})$. Thus, the matrix elements $s_{\lambda, i\alpha}$ in equation (35) can readily be determined by inverting the matrix with elements $t_{i\alpha, \mu}$ or, equivalently, by solving the system of linear equations (37). The choice of linearized vibrational coordinates provides a simple form for $t_{i\alpha, \mu}$. Had we chosen geometrically defined, internal vibrational coordinates (i.e., bond lengths and interbond angles) as generalized coordinates, the elements of $t_{i\alpha, \mu}$ would be more complicated, but the approach for obtaining $s_{\lambda, i\alpha}$, which we describe below, would still be applicable.

At this point we choose to introduce linearized Morse variables $y_k^\ell = 1 - \exp(-a \Delta r_k^\ell)$ $(k = 1, 2, 3)$, where a is the range parameter of the Morse potential. These variables simplify the computation of the matrix elements required for the variational calculation. Morse oscillator basis functions are used in setting up the Hamiltonian matrix; these functions provide a rather good description of stretching motion [13] and allow us to express the potential energy function as a low-order power series expansion. All analytical functions in the rotational–vibrational

Hamiltonian are expanded as power series in the vibrational variables

$$\xi_n^\ell = \left(y_1^\ell, y_2^\ell, y_3^\ell, S_{4a}, S_{4b}\right), \tag{45}$$

i.e. linearized Morse variables and linearized symmetrized bending coordinates. These coordinates are also employed for solving equation (37).

Generally, it is not a trivial problem to invert the matrix with elements $t_{i\alpha,\mu}$. We cannot, in practice, determine an analytical solution of equation (37) and so we solve it numerically. The system of equations (37) consists of $(3N)^2 = 144$ equations involving 144 variables $t_{i\alpha,\mu}$, which can easily be reduced by taking into account the properties of the coordinate transformation. The translational, vibrational and rotational parts of equation (37) are separable, and there is no intermode interaction in the matrix with elements $t_{i\alpha,\mu}$. Consequently, equation (37) can be solved for each mode λ independently. This leaves us with 12 sets, labeled by $\mu = 1 \ldots 12$, each set with $3N = 12$ independent equations which define $3N = 12$ matrix elements $s_{i\alpha,\lambda}$, $i = 1, 2, 3, 4$ and $\alpha = x, y, z$. However this is still a complicated problem to solve analytically. In order to solve it numerically, we expand the $t_{i\alpha,\mu}$ and $s_{\lambda,i\alpha}$ matrix elements as power series in the ξ_n^ℓ coordinates defined above:

$$t_{i\alpha,\mu}(\xi_n^\ell) = \sum_{L\geq 0}\sum_{L[l]} t_{L[l]}^{i\alpha,\mu}\,(\xi^\ell)^{L[l]}, \tag{46}$$

$$s_{\lambda,i\alpha}(\xi_n^\ell) = \sum_{L\geq 0}\sum_{L[l]} s_{L[l]}^{\lambda,i\alpha}\,(\xi^\ell)^{L[l]}, \tag{47}$$

where we introduced the notation

$$\sum_{L[l]} f_{L[l]}(x)^{L[l]} \equiv \sum_{l_1=0}^{L}\sum_{l_2=0}^{(L-l_1)}\sum_{l_3=0}^{(L-l_1-l_2)}\sum_{l_{4a}=0}^{(L-l_1-l_2-l_3)} f^{L}_{l_1 l_2 l_3 l_{4a} l_{4b}} \times x_1^{l_1} x_2^{l_2} x_3^{l_3} x_{4a}^{l_{4a}} x_{4b}^{l_{4b}}, \tag{48}$$

with $l_{4b} = L - l_1 - l_2 - l_3 - l_{4a}$. We end up with a system of *linear* equations of the type $\mathbf{Tx} = \mathbf{b}$:

$$\sum_{i\alpha} t_{0[0]}^{i\alpha,\mu}\, s_{0[0]}^{\lambda,i\alpha} = \delta_{\lambda,\mu}, \tag{49}$$

$$\sum_{i\alpha} t_{0[0]}^{i\alpha,\mu}\, s_{L[l]}^{\lambda,i\alpha} = b_{L[l]}^{\mu,\lambda}, \quad L > 0, \tag{50}$$

where

$$b_{L[l]}^{\mu,\lambda} = -\sum_{K=0}^{L-1}\sum_{K[k]}\sum_{i\beta} t_{(L-K)[l-k]}^{i\beta,\mu}\, s_{K[k]}^{\lambda,i\beta}. \tag{51}$$

Each set of equations given in (49) and (50) is represented by the 12×12 coefficient matrix $\mathbf{T}$ with elements $t_{0[0]}^{i\alpha,\mu}$, which is common for all orders of magnitude L, and by the 12-dimensional 'right-hand-side' vector $\mathbf{b}_{L[\lambda]}^{\mu}$ with elements $b_{L[l]}^{\mu,1}$; this vector is recursively determined at each order. Thus, for every mode λ at each iteration step L, there are $12 \times (L+4)(L+3)(L+2)(L+1)/24$ independent sets of 12 equations for 12 independent variables $x_{i\alpha} = s_{L[l]}^{\lambda,i\alpha}$. If we know the solution of equation (50) up to and including order L we can derive recursively the matrix elements $s_{L+1[l]}^{\lambda,i\alpha}$ for order $(L+1)$. We should bear in mind that all quantities $t_{(L-K)[l-k]}^{i\beta,\mu}$ and $s_{K[k]}^{\lambda,i\beta}$ are functions of ρ. Therefore, we construct a discrete grid of equidistantly spaced ρ-values ρ_k and solve the system of linear equations (49–50) at each ρ_k point. The matrix elements $s_{\lambda,i\alpha}$ are obtained as expansions in the ξ_n^ℓ coordinates at the non-rigid reference configuration.

The expansion coefficients $G_{\lambda,\mu}$ in the kinetic energy operator [equation (42)] are expressed as power series in the ξ_n coordinates:

$$G_{\lambda,\mu}(\xi_n^\ell, \rho) = \sum_{L\geq 0}\sum_{L[l]} G_{L[l]}^{\lambda,\mu}(\rho)\,(\xi_n^\ell)^{L[l]} \tag{52}$$

and, from equation (43) and the known expansions of the $s_{\lambda,i\alpha}$ matrix elements, the expansion coefficients are obtained as

$$G_{L[l]}^{\lambda,\mu}(\rho) = \sum_{i\beta}\frac{1}{m_i}\sum_{K=0}^{L}\sum_{K[k]} s_{(L-K)[l-k]}^{\lambda,i\beta}(\rho)\, s_{K[k]}^{\mu,i\beta}(\rho). \tag{53}$$

It should be emphasized that we do not derive any analytical expressions for the ρ-dependent functions considered here except in rather trivial cases, such as the vector components $a_{i\alpha}(\rho)$ and the matrix elements $A_{i\alpha,n}(\rho)$. The two-line recursion relations (49) and (50) replace thousands of lines with the corresponding analytical expressions. No additional analytical derivations or tiresome expressions are required. The kinetic energy operator is entirely defined by the recursion procedure in equations (49, 50) so that it is a trivial task to implement it as computer code. In our current realization of the procedure given in equations (49, 50), the expansions in equations (46, 47) can have a maximum order of eight.

The strategy chosen for solving the rotational-vibrational Schrödinger equation (i.e. to obtain a matrix representation of the rotation–vibration Hamiltonian that we can diagonalize) is the logical consequence of the procedure developed in the present section. All ρ–dependent functions in the Hamiltonian are represented as power series expansions in the ξ_n^ℓ coordinates

around the reference configuration. The expansion coefficients depend on ρ and are represented as a table of numerical values determined at a grid of equidistantly spaced ρ-values ρ_k. All matrix element integration over ρ is done numerically by means of Simpson's rule.

4. Quantum-mechanical kinetic operator

We quantize the classical kinetic energy in equation (42) by the methods described in [33, 34]. The momentum transformation (34) in symmetrized form is given by:

$$\mathbf{P}_i = \frac{1}{2}\sum_{\lambda=1}^{3N}(\mathbf{s}_{\lambda,i}\,\Pi_\lambda + \Pi_\lambda\,\mathbf{s}_{\lambda,i}) \tag{54}$$

where $\mathbf{P}_i$ has the components (P_{iX}, P_{iY}, P_{iZ}) and $\mathbf{s}_{\lambda,i}$ has the components $(s_{\lambda,iX}, s_{\lambda,iY}, s_{\lambda,iZ})$. Equation (54) is the quantum mechanical replacement for the classical equation (34). By inserting equation (54) in equation (42) and taking into account relations (40), we obtain the quantum-mechanical kinetic energy operator [33, 34]:

$$\hat{T} = \frac{1}{2}\sum_{\lambda=1}^{3N}\sum_{\mu=1}^{3N}\Pi_\lambda\,G_{\lambda,\mu}\,\Pi_\mu + U(\xi_n^\ell,\rho); \tag{55}$$

where $G_{\lambda,\mu}$ are determined by equation (43) and

$$U = \sum_{\lambda=1}^{3N}\sum_{\lambda'=1}^{3N}\sum_{i=1}^{N}\left\{\frac{1}{8}\,m_i^{-1}\left[\Pi_\lambda,\mathbf{s}_{\lambda,i}\right]\cdot\left[\Pi_{\lambda'},\mathbf{s}_{\lambda',i}\right] + \frac{1}{4}\,m_i^{-1}\,\mathbf{s}_{\lambda,i}\cdot\left[\Pi_\lambda,[\Pi_{\lambda'},\mathbf{s}_{\lambda',i}]\right]\right\}. \tag{56}$$

The pseudopotential term U is expressed in terms of commutators between the conjugate momenta and the transformation vectors. It can be included in the potential energy function.

Employing the recursion procedure in equations (49, 50), the pseudopotential function U is expressed in terms of the five linearized vibrational coordinates ξ_n^ℓ and the curvilinear ρ coordinate analogous to expansion (52), and truncated at the same order as the $G_{\lambda,\mu}$ terms.

5. Potential energy function

We distinguish two types of potential energy surface representations here. Type A is defined in terms of geometrically defined, internal coordinates. It is designed with the sole purpose of representing the potential energy surface in the best possible way; its form has no direct relation to the variational problem and can, at least in principle, be chosen freely. Usually it is taken to be isotope independent. A Type B representation defines the potential energy surface in terms of our non-rigid reference configuration [see equation (1)] and is not isotope independent. It is expanded as a power series in the linearized coordinates ξ_n^ℓ for a particular value of ρ. The expansion coefficients are ρ-dependent and we express them as a table of numerical values determined at a grid of equidistantly spaced ρ-values ρ_k, exactly as done for the ρ-dependent functions in the kinetic energy operator. The Type B expansion is designed to simplify the calculation of Hamiltonian matrix elements in the subsequent variational calculations.

In the present work, we initially employ a Type A expansion of the potential energy surface for the electronic ground state of NH_3

$$\begin{aligned}V(\xi_1,\xi_2,\xi_3,\xi_{4a},\xi_{4b};\sin\bar{\rho}) &= V_0(\sin\bar{\rho}) + \sum_j F_j(\sin\bar{\rho})\,\xi_j + \sum_{j\le k}F_{jk}(\sin\bar{\rho})\,\xi_j\,\xi_k \\ &+ \sum_{j\le k\le l}F_{jkl}(\sin\bar{\rho})\,\xi_j\,\xi_k\,\xi_l + \sum_{j\le k\le l\le m}F_{jklm}(\sin\bar{\rho}) \\ &\times \xi_j\,\xi_k\,\xi_l\,\xi_m\ldots.\end{aligned} \tag{57}$$

This analytical function [1] is expressed in terms of the variables

$$\xi_k = 1 - \exp\left(-a(r_k - r_e)\right),\quad k = 1,2,3, \tag{58}$$

$$\xi_{4a} = \frac{1}{\sqrt{6}}\,(2\alpha_{23} - \alpha_{13} - \alpha_{12}), \tag{59}$$

$$\xi_{4b} = \frac{1}{\sqrt{2}}\,(\alpha_{13} - \alpha_{12}), \tag{60}$$

$$\sin\bar{\rho} = \frac{2}{\sqrt{3}}\sin(\bar{\alpha}/2), \tag{61}$$

where $\bar{\alpha} = (\alpha_{12} + \alpha_{23} + \alpha_{13})/3$ is the average of the interbond angles. The variable $\sin\bar{\rho}$ is of A_1 symmetry in $\mathcal{D}_{3h}(M)$, by definition, and coincides with $\sin\rho$ at the reference configuration. We use $\sin\bar{\rho}$ only for the representation of the potential energy surface, and hence we never require the value of $\bar{\rho}$.

The pure inversion potential energy function in equation (57) is

$$V_0(\sin\bar{\rho}) = \sum_s f_0^{(s)}(\sin\rho_e - \sin\bar{\rho})^s, \tag{62}$$

and the functions $F_{jk...}(\sin\bar{\rho})$ are defined as

$$F_{jk...}(\sin\bar{\rho}) = \sum_s f_{jk...}^{(s)} (\sin\rho_e - \sin\bar{\rho})^s, \qquad (63)$$

where ρ_e is the equilibrium value[2] of ρ, a is a molecular parameter, and the quantities $f_0^{(s)}$ and $f_{jk...}^{(s)}$ in equations (62) and (63) are expansion coefficients. The analytical function in equation (57) is similar to the expansion introduced for triatomic molecules in [12].

By expressing V as an expansion in $\sin\bar{\rho}$, we ensure that, as required by symmetry, the potential energy function always has a maximum or a minimum at planar configurations. Further, V is totally symmetric under the operations in the MS group $\mathcal{D}_{3h}(M)$, and this imposes relations between the $f_{jk...}^{(s)}$ parameters in equation (63).

The kinetic energy operator described in section 4 is expressed in terms of the generalized coordinates from equation (31) and the quantum mechanical form of the momenta from equation (32). In order to obtain a useful Hamiltonian with this kinetic energy operator, we must transform the Type A representation of the potential energy function in equation (57) to a Type B representation that depends on the generalized coordinates from equation (31). The corresponding coordinate transformation is done in three steps:

$$\{\xi_n, \sin\bar{\rho}\} \overset{(a)}{\rightarrow} \{r_1, r_2, r_3, \alpha_{23}, \alpha_{13}, \alpha_{12}\} \overset{(b)}{\rightarrow} \{R_{i,\beta}\} \overset{(c)}{\rightarrow} \{\xi_n^\ell, \rho\}. \qquad (64)$$

In transformation (a) the geometrically defined coordinates from equations (58–60) are expanded in terms of the bond lengths and interbond angles; in transformation (b) these latter coordinates are expanded in terms of the xyz Cartesian displacement coordinates by using equations (19, 20), and finally in transformation (c) the linearized coordinates are introduced by means of equations (1, 26). The resulting Type B representation of the potential energy surface is expressed in a form similar to equation (57), where the expansion coefficients parameters $F_{jk...}^\ell(\rho)$ are given as tables of numerical values determined at the grid of equidistantly spaced ρ-values ρ_k. Our current code allows a 6th order expansion in the ξ_n^ℓ variables for the Type B potential function.

We generally follow a strategy of avoiding complicated analytical derivations and, for the transformation $V(\xi_n, \sin\bar{\rho}) \rightarrow V(\xi_n^\ell, \rho)$, this means that we calculate the coefficients $F_{ijk...}^\ell(\rho)$ numerically by a 4-point finite-difference expression. This is a universal procedure, independent of the form of the Type A representation for the potential energy function employed. As long as the particular choice of the geometrically defined, internal coordinates can be related to the Cartesian coordinates, we can always expand $V(\xi_n^\ell, \rho)$ by means of the finite-difference method. The disadvantage of the numerical procedure is the error introduced by the finite differences. Alternatively, the parameters $F_{ijk...}^\ell(\rho)$ could be obtained in least-squares fittings, either to potential energy values generated from a Type A representation, or directly to the *ab initio* data. Such fittings would have to be carried out for each isotopomer separately.

6. Basis set

Aiming at solving the rotational-vibrational Schrödinger equation variationally, we construct the rovibrational basis functions as symmetrized linear combinations of primitive-basis-function products:

$$|J, m, N_{vir}\Gamma_{vir}\rangle = [|J, K, m, \tau_{rot}\rangle \times |n_i, J, K, \tau_{inv}\rangle |n_b, l_b, \tau_{bend}\rangle |n_1\rangle |n_2\rangle |n_3\rangle]^{\Gamma_{vir}}, \qquad (65)$$

where $|n_1\rangle$, $|n_2\rangle$, and $|n_3\rangle$ are one-dimensional Morse-oscillator eigenfunctions [40], $|n_b, l_b, \tau_{bend}\rangle$ are 2D isotropic-harmonic-oscillator functions, $|n_i, J, K, \tau_{inv}\rangle$ are Numerov-Cooley eigenfunctions of the one-dimensional inversion Schrödinger equation (see below), and $|J, K, m, \tau_{rot}\rangle$ are rigid symmetric rotor wavefunctions. The symbol Γ_{vir} represents one of the irreducible representations of $\mathcal{D}_{3h}(M)$ contained in the representation spanned by the function product in equation (65) (see [31]), and the quantum number N_{vir} enumerates basis functions with the same J and Γ_{vir}.

6.1. *Rotational basis functions*

The rotational basis set is represented by usual rigid symmetric rotor wavefunctions $|J, k, m\rangle$ (see, for example, [31]). The quantum numbers J, $k = -J \ldots J$ and $m = -J \ldots J$ are associated with the total angular momentum, its projection onto the z axis and its projection onto the Z axis, respectively. The symmetrized linear combinations $|J, K, m, \tau_{rot}\rangle$ are identical to those used in [40]. They provide a real matrix

[2] Since the equilibrium geometry is a reference configuration, $\sin\bar{\rho}$ and $\sin\rho$ have the same equilibrium value $\sin\rho_e$.

representation of the kinetic energy operator in equation (55) and are given by

$$|J,0,m,\tau_{\rm rot}\rangle = i^{\tau_{\rm rot}}|J,0,m\rangle, \quad \tau_{\rm rot} = J \bmod 2, \tag{66}$$

$$|J,K,m,\tau_{\rm rot}\rangle = \frac{i^{\tau_{\rm rot}}(-1)^{\sigma_{\rm rot}}}{\sqrt{2}}\big(|J,K,m\rangle + (-1)^{J+K+\tau_{\rm rot}} |J,-K,m\rangle\big), \tag{67}$$

where $\tau_{\rm rot} = 0, 1$ indicates the rotational parity $(-1)^{\tau_{\rm rot}}$, $\sigma_{\rm rot} = K \bmod 3$ for $\tau_{\rm rot} = 1$, and $\sigma_{\rm rot} = 0$ for $\tau_{\rm rot} = 0$, and $K = 0 \ldots J$. The phases in equations (66, 67) are chosen as in [8]. The symmetry $\Gamma_{\rm rot}$ of the rotational function $|J,K,m,\tau_{\rm rot}\rangle$ is given as

$$\begin{aligned} |J,K=3t,m,\tau_{\rm rot}=0\rangle &\to A_1^\dagger \\ |J,K=3t,m,\tau_{\rm rot}=1\rangle &\to A_2^\dagger \\ |J,K\neq 3t,m,\tau_{\rm rot}=0\rangle &\to E_a^\dagger \\ |J,K\neq 3t,m,\tau_{\rm rot}=1\rangle &\to E_b^\dagger \end{aligned} \tag{68}$$

where t is a positive integer number, $\dagger = '$ if K is even, and $\dagger = ''$ when K is odd.

6.2. *Inversion basis functions*

The inversion wavefunctions $|n_{\rm i},J,K,\tau_{\rm inv}\rangle$ are obtained as numerical solution of the pure inversion one-dimensional Schrödinger equation:

$$\begin{aligned} H^0_{\rm (inv)} = &-\frac{1}{2}\frac{\partial}{\partial\rho}G^0_{\rho,\rho}(\rho)\frac{\partial}{\partial\rho} + \frac{1}{4}\Big[G^0_{x,x}(\rho) + G^0_{y,y}(\rho)\Big] \\ &\times\big[J(J+1) - K^2\big] + \frac{1}{2}G^0_{z,z}K^2 \\ &+ V_0(\rho) + U(\xi^\ell_n = 0, \rho), \end{aligned} \tag{69}$$

obtained by neglecting, in the complete rovibrational Hamiltonian, the small-amplitude displacements from the reference configuration (see [6]). In equation (69) we introduced the notation $G^0_{\lambda,\lambda}(\rho) \equiv G_{\lambda,\lambda}(\xi^\ell_n = 0, \rho)$. The one-dimensional Schrödinger equation obtained from equation (69) is solved by the numerical Numerov-Cooley integration method [41, 42] as detailed in [11]. The Hamiltonian $H^0_{\rm (inv)}$ depends parametrically on the rotational quantum numbers J and K, i.e. the effective inversion potential is different for each rotational state. The eigenfunctions of equation (69), being stationary solutions, are labeled by the inversion quantum number $n_{\rm i}$ and by the parity parameter $\tau_{\rm inv}$. The parity is $(-1)^{\tau_{\rm inv}}$ so that for $\tau_{\rm inv} = 0(1)$ the primitive inversion basis function is unchanged (changed in sign) by the inversion operation E^* which takes ρ into $\pi - \rho$. Positive parity is associated with A_1' symmetry in $\mathcal{D}_{3\rm h}$(M), negative parity with A_2'' symmetry.

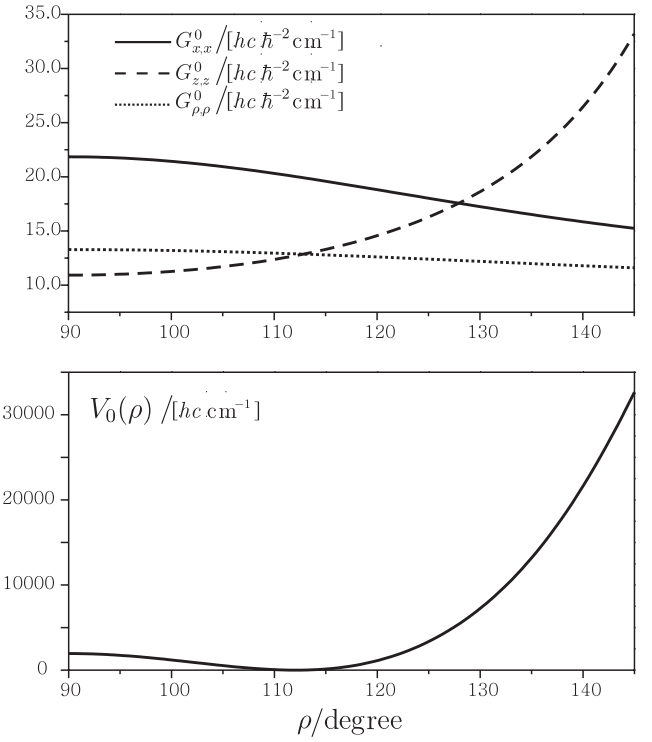

Figure 2. The ρ-dependent functions $G^0_{x,x}(\rho)$, $G^0_{z,z}(\rho)$, $G^0_{\rho,\rho}(\rho)$, and $V_0(\rho)$.

It is known from MORBID studies of triatomic molecules [12] that the J,K-parametrization of the primitive bending wavefunctions allows one to reduce effectively the configuration space at the diagonalization stage of the variational problem. In case of triatomics it is crucial to include the K-dependent terms with the bending motion because the $G_{z,z}$ term is singular at linearity [11]. The importance of the K-terms for NH_3 is also apparent from the relatively strong ρ-dependence of $G^0_{z,z}$, even though it is not singular at any geometry. This statement is illustrated by figure 2, where the $G^0_{x,x}$, $G^0_{z,z}$, $G^0_{\rho,\rho}$, and $V_0(\rho)$ functions are plotted against ρ.

The numerical eigenfunctions of the Hamiltonian in equation (69) and their first derivatives are stored as tables of numerical values determined at the grid of $N_{\rm inv}$ equidistantly spaced ρ-values ρ_k. The first derivatives are needed for the computation of matrix elements of the Hamiltonian terms $J_\rho\, G_{\rho,\lambda}(\rho)$, $G_{\lambda,\rho}(\rho)\, J_\rho$, and $J_\rho\, G_{\rho,\rho}(\rho)\, J_\rho$ [equation (55)].

6.3. *Bending basis functions*

The bending coordinates S_{4a} and S_{4b} transform according to the degenerate irreducible representation E' of $\mathcal{D}_{3\rm h}$(M), and so we choose the eigenfunctions

of a two-dimensional, isotropic harmonic oscillator as the basis functions associated with them. Since the Hamiltonian is Hermitian, we can obtain a real matrix representation by using real harmonic-oscillator eigenfunctions involving $\cos(l_b\varphi)$ and $\sin(l_b\varphi)$, rather than the usual complex form involving $\exp(il_b\varphi)$ [43]. The positive-parity functions ($\tau_{bend}=0$), expressed in terms of polar coordinates $\{r_4,\varphi\}$, are given by:

$$|n_b, l_b, 0\rangle = N_{n_b,l_b}\exp(-r_4^2/2)\, r_4^{l_b}\, L^{l_b}_{(n_b-l_b)/2}(r_4^2)\cos(l_b\varphi) \tag{70}$$

and the negative-parity functions ($\tau_{bend}=1$) are:

$$|n_b, l_b, 1\rangle = (-1)^{\sigma_b} N_{n_b,l_b} \times \exp(-r_4^2/2)\, r_4^{l_b}\, L^{l_b}_{(n_b-l_b)/2}(r_4^2)\sin(l_b\varphi), \tag{71}$$

where $L_k^{l_b}$ is a generalized Laguerre polynomial [44], n_b is the principal vibrational quantum number, l_b is the vibrational angular momentum quantum number, and $\sigma_b = l_b \bmod 3$. The normalization constant is

$$N_{n_b,l_b} = \sqrt{2-\delta_{l_b,0}}\sqrt{\frac{[(n_b-l_b)/2]!}{\pi[(n_b+l_b)/2]!}} \tag{72}$$

and the dimensionless normal coordinates are given by:

$$Q_{4a} = r_4\cos(\varphi) = \left(\frac{2f^{\,0}_{4a4a}}{G^0_{4a,4a}(\rho_e)}\right)^{1/4}\times S_{4a} \tag{73}$$

$$Q_{4b} = r_4\sin(\varphi) = \left(\frac{2f^{\,0}_{4a4a}}{G^0_{4a,4a}(\rho_e)}\right)^{1/4}\times S_{4b}, \tag{74}$$

where $\omega_b = [2f^{\,0}_{4a4a}G^0_{4a,4a}(\rho_e)]^{1/2}$ is the vibrational frequency of the two-dimensional isotropic harmonic oscillator and $G^0_{4a,4a}(\rho_e) = G_{4a,4a}(\xi^\ell_n=0,\rho=\rho_e)$. The vibrational angular momentum l_b can only take positive values $n_b, n_b-2,\ldots,1$ or 0. The eigenvalues are independent of l_b so that an energy level with a given value of n_b is (n_b+1)-fold degenerate. The constructed bending basis functions have the following symmetry properties:

$$\begin{aligned}
&|n_b,\, l_b=0,\ \ \tau_{bend}=0\rangle \to A_1'\\
&|n_b,\, l_b=3t,\ \tau_{bend}=0\rangle \to A_1'\\
&|n_b,\, l_b=3t,\ \tau_{bend}=1\rangle \to A_2'\\
&|n_b,\, l_b\neq 3t,\ \tau_{bend}=0\rangle \to E_a'\\
&|n_b,\, l_b\neq 3t,\ \tau_{bend}=1\rangle \to E_b'.
\end{aligned} \tag{75}$$

where the two components of E' (see table 1) are labeled E_a' and E_b', respectively.

6.4. *Stretching basis set*

The Morse potential

$$V_{Morse}(r) = D\,y^2 = D\,[1-\exp(-a\Delta r)]^2 \tag{76}$$

models the potential energy curves of many diatomic molecules very well [45], and therefore it is also used to describe stretching motion in polyatomic systems (see, for example, [13]). In equation (76), r is the internuclear distance describing the stretching motion and $\Delta r = r - r_e$ is the displacement from the equilibrium value r_e, D is the dissociation energy, a is a parameter determining the curvature of the potential at $r=r_e$, and $y = 1-\exp(-a\Delta r)$. A stretching potential energy surface represented in terms of Morse variables y has obvious mathematical advantages, such as good convergence properties and simple analytical expressions for matrix elements between Morse oscillator eigenfunctions.

The Morse oscillator eigenfunctions $|n\rangle$ are solutions of the one-dimensional Schrödinger equation with the Morse potential:

$$\left[-\frac{\hbar^2}{2\mu}\frac{\partial^2}{\partial r^2} + Dy^2\right]|n\rangle = E_n|n\rangle, \tag{77}$$

where μ is the reduced mass of the system and $|n\rangle$ is expressed in terms of generalized Laguerre polynomials (see [44]). The stretching basis functions are constructed as the products $|n_1\rangle|n_2\rangle|n_3\rangle$. It should be noted that the Morse oscillator eigenfunctions used as basis functions here depend on the *linearized* stretching coordinates Δr_1^ℓ, Δr_2^ℓ, Δr_3^ℓ, rather than on the usual, geometrically defined bond length displacements.

7. Symmetry factorization of the Hamiltonian matrix

The variational solution of the fully-dimensional rotation-vibration Schrödinger equation for a four-atomic molecule is a formidable numerical problem, involving the diagonalization of huge matrices. Therefore it is essential to take advantage of the high intrinsic symmetry of pyramidal XY_3 molecules. The Hamiltonian matrix is diagonal in the total angular momentum quantum number J, and when we employ basis functions symmetrized in $\mathcal{D}_{3h}(M)$, each J-block becomes block diagonal with a sub-block for each irreducible representation of $\mathcal{D}_{3h}(M)$ [31]. The sub-blocks can be diagonalized separately and so we can effectively reduce the sizes of the matrices that need to be diagonalized. In addition, each of the degenerate irreducible representations E' and E'' gives rise to two

sub-blocks with identical eigenvalues so that it is sufficient to diagonalize only one of these.

The eigenvalue problem is solved as follows. The matrix elements $H_{k,l}$ of the total rotation–vibration Hamiltonian are first calculated in terms of primitive basis functions

$$\varphi^{[r]} = \underbrace{|J, K, m, \tau_{rot}\rangle}_{\text{rotation}} \underbrace{|n_i, J, K, \tau_{inv}\rangle}_{\text{inversion}} \underbrace{|n_b, l_b, \tau_{bend}\rangle}_{\text{bending}} \underbrace{|n_1\rangle|n_2\rangle|n_3\rangle}_{\text{stretching}} \tag{78}$$

that transform according to reducible representations of $\mathcal{D}_{3h}(M)$. Then the matrix with elements $H_{k,l}$ is transformed to the block-diagonal form associated with the symmetrized basis functions $\psi_\alpha^{[irr],\Gamma}$ (where 'irr' stands for '*irreducible representation*,' Γ is the MS group symmetry of the basis function, and α labels functions with the same Γ). Towards this end, we perform an orthogonal transformation to the symmetrized basis functions by means of projection operators $\hat{P}^\Gamma$ [31]:

$$\psi_\alpha^{[irr],\Gamma} = \hat{P}^\Gamma \varphi^{[r]}. \tag{79}$$

It is not necessary to calculate and transform the whole primitive matrix of elements $H_{k,l}$ in one fell swoop. The primitive basis functions can be sorted into relatively small sets, each of which spans a reducible representation of $\mathcal{D}_{3h}(M)$. For example, the primitive stretching basis functions $|n\rangle|0\rangle|0\rangle$, $|0\rangle|n\rangle|0\rangle$ and $|0\rangle|0\rangle|n\rangle$ span the three-dimensional reducible representation $A_1' \oplus E'$ of $\mathcal{D}_{3h}(M)$ [31]. From these three primitive basis functions, we obtain the symmetrized functions

$$\psi^{A_1'} = (|0\rangle|0\rangle|n\rangle + |n\rangle|0\rangle|0\rangle + |0\rangle|n\rangle|0\rangle)/\sqrt{3}, \tag{80}$$

$$\psi^{E_a'} = (2|0\rangle|0\rangle|n\rangle - |n\rangle|0\rangle|0\rangle - |0\rangle|n\rangle|0\rangle)/\sqrt{6}, \tag{81}$$

$$\psi^{E_b'} = (|n\rangle|0\rangle|0\rangle - |0\rangle|n\rangle|0\rangle)/\sqrt{2}. \tag{82}$$

In general, any combination of indexes $\{JK; n_1 \geq n_2 \geq n_3; n_b l_b; n_i\}$ is associated with a set of primitive basis functions

$$\begin{bmatrix} |J,\ K,\ m, 0\rangle \\ |J,\ K,\ m, 1\rangle \end{bmatrix} \times \begin{bmatrix} |n_i, J, K, 0\rangle \\ |n_i, J, K, 1\rangle \end{bmatrix} \times \begin{bmatrix} |n_b, l_b, 0\rangle \\ |n_b, l_b, 1\rangle \end{bmatrix} \times \begin{bmatrix} |n_1\rangle|n_2\rangle|n_3\rangle \\ |n_2\rangle|n_3\rangle|n_1\rangle \\ |n_3\rangle|n_1\rangle|n_2\rangle \\ |n_1\rangle|n_3\rangle|n_2\rangle \\ |n_2\rangle|n_1\rangle|n_3\rangle \\ |n_3\rangle|n_2\rangle|n_1\rangle \end{bmatrix} \tag{83}$$

which span an N_r-dimensional reducible representation of $\mathcal{D}_{3h}(M)$. There are at most (when n_1, n_2, n_3 are all different) 48 basis functions in the set defined by equation (83). However, these can be separated into 24 functions with positive parity ($\tau_{rot} + \tau_{inv} + \tau_{bend}$ even) and 24 functions with negative parity ($\tau_{rot} + \tau_{inv} + \tau_{bend}$ odd). Thus, in constructing symmetrized basis functions, we must consider at most 24 primitive basis functions simultaneously.

The elements of the representation matrices generated by the set of functions in equation (83) are obtained as

$$D^{riv}[R]_{ijk,i'j'k'} = D^{(rot)}_{ii'}[R]\, D^{(inv)}_{jj'}[R]\, D^{(vib)}_{kk'}[R], \tag{84}$$

where R is a group operation and $D^{(rot)}_{ii'}[R]$, $D^{(inv)}_{jj'}[R]$, and $D^{vib}_{kk'}[R]$ are elements of the representation matrices generated by the primitive basis functions describing rotation, inversion, and small-amplitude vibration (bending and stretching), respectively. These matrices are determined as described in [31]. The indices i and i' label the primitive rotational basis functions, j and j' label the primitive inversion basis functions, and k and k' label the primitive small-amplitude vibration basis functions. The quantity $D^{riv}[R]_{ijk,i'j'k'}$ in equation (84) is, in this labeling, an element of a representation matrix generated by the function products defined in equation (83). The corresponding representation has the characters

$$\chi^{(riv)}[R] = \chi^{(rot)}[R]\, \chi^{(inv)}[R]\, \chi^{(vib)}[R] \tag{85}$$

and can be reduced in terms of irreducible representations by means of equation (5–45) of [31].

We obtain a symmetrized basis function $\psi_\alpha^{[irr],\Gamma}$ by applying [equation (79)] the projection operator $\hat{P}^\Gamma$ to the primitive basis function $\varphi^{[r]}$ which, in an obvious notation, can be written as

$$\varphi^{[r]} = \Phi^{(riv)}_{ijk} = \Phi^{(rot)}_i\, \Phi^{(inv)}_j\, \Phi^{(vib)}_k. \tag{86}$$

We express $\psi_\alpha^{[irr],\Gamma}$ in terms of the primitive basis functions as

$$\psi_\alpha^{[irr],\Gamma} = \hat{P}^\Gamma\, \Phi^{(riv)}_{ijk} = \sum_{i'j'k'} P^\Gamma_{\alpha,i'j'k'}\, \Phi^{(riv)}_{i'j'k'}. \tag{87}$$

For the non-degenerate irreducible representations of $\mathcal{D}_{3h}(M)$, $\Gamma = A_1', A_2', A_1''$, or A_2'', it follows from equation (6–67) of [31] that

$$P^\Gamma_{\alpha,i'j'k'} = \frac{1}{12} \sum_R \chi^\Gamma[R]^*\, D^{riv}[R]_{ijk,i'j'k'}. \tag{88}$$

Projecting to the doubly degenerate representations E' and E'' is more tricky. We use equation (6–64) of [31] to obtain

$$\tilde{P}^{E_a}_{\alpha,\,i'j'k'} = \frac{2}{12}\sum_R D^{(E)}[R]^*_{11}\, D^{\mathrm{riv}}[R]_{ijk,\,i'j'k'}, \qquad (89)$$

$$\tilde{P}^{E_b}_{\alpha,\,i'j'k'} = \frac{2}{12}\sum_R D^{E}[R]^*_{22}\, D^{\mathrm{riv}}[R]_{ijk,\,i'j'k'}, \qquad (90)$$

where $D^{(E)}[R]_{11}$ and $D^{E}[R]_{22}$ are the diagonal elements of representation matrices associated with the E irreducible representation in question. If the two symmetrized basis functions obtained in this way are not orthogonal, they can be orthogonalized by standard Schmidt orthogonalization [31].

The elements $H^{\Gamma}_{\alpha',\alpha''}$ of the block diagonal, 'symmetrized' matrix are given in terms of the elements $H_{i'j'k',\,i''j''k''}$ of the original, 'primitive' matrix:

$$H^{\Gamma}_{\alpha',\alpha''} = \sum_{i'j'k'}\sum_{i''j''k''}\left(P^{\Gamma}_{\alpha',\,i'j'k'}\right)^* H_{i'j'k',\,i''j''k''}\, P^{\Gamma}_{\alpha'',\,i''j''k''}. \qquad (91)$$

8. Computational details

As described in sections 4 and 5, we expand the rotation–inversion–vibration Hamiltonian $\widehat{H}_{riv}$ in the variables given in equations (45) and so we can write it symbolically as

$$\widehat{H}_{riv} = \sum_p \widehat{O}^{(p)}_{\mathrm{r}}\,\widehat{O}^{(p)}_{\mathrm{i}}\,\widehat{O}^{(p)}_{\mathrm{b}}\,\widehat{O}^{(p)}_{\mathrm{s}} \qquad (92)$$

where the rotational operator $\widehat{O}^{(p)}_{\mathrm{r}}$ depends on the Euler angles θ, ϕ, χ through the components of the total angular momentum, the inversion operator $\widehat{O}^{(p)}_{\mathrm{i}}$ depends on ρ and $\hat{J}_\rho$, the bending operator $\widehat{O}^{(p)}_{\mathrm{b}}$ depends on $(S^{\ell}_{4a}, S^{\ell}_{4b})$ and their conjugate momenta, and finally the stretching operator $\widehat{O}^{(p)}_{\mathrm{s}}$ depends on $(\Delta r^{\ell}_1, \Delta r^{\ell}_2, \Delta r^{\ell}_3)$ and their conjugate momenta. The summation index p labels the different terms in the Hamiltonian.

A matrix element of one term in equation (92) between two of the primitive basis functions given in equation (65) is obviously a product of four distinct integrals involving different coordinates: $\langle J, K'', m, \tau''_{\mathrm{rot}}|\widehat{O}^{(p)}_{\mathrm{r}}|J, K', m, \tau'_{\mathrm{rot}}\rangle$, $\langle n''_{\mathrm{i}}, J, K'', \tau''_{\mathrm{inv}}|\widehat{O}^{(p)}_{\mathrm{i}}|n'_{\mathrm{i}}, J, K', \tau'_{\mathrm{inv}}\rangle$, $\langle n''_{\mathrm{b}}, l''_{\mathrm{b}}, \tau''_{\mathrm{bend}}|\widehat{O}^{(p)}_{\mathrm{b}}|n'_{\mathrm{b}}, l'_{\mathrm{b}}, \tau'_{\mathrm{bend}}\rangle$, and $\langle n''_1|\langle n''_2|\langle n''_3|\widehat{O}^{(p)}_{\mathrm{s}}|n'_1\rangle|n'_2\rangle|n'_3\rangle$.

The matrix elements $\langle J, K'', m, \tau''_{\mathrm{rot}}|\widehat{O}^{(p)}_{\mathrm{r}}|J, K', m, \tau'_{\mathrm{rot}}\rangle$ involving symmetrized rotational wavefunctions can be obtained by making suitable transformations of the matrix elements calculated in terms of unsymmetrized rigid rotor functions $|J, k, m\rangle$; these latter matrix elements are given, for example, in [8]. The rotational matrix elements are diagonal in J and m, and they do not depend on m.

The inversion matrix elements $\langle n''_{\mathrm{i}}, J, K'', \tau''_{\mathrm{inv}}|\widehat{O}^{(p)}_{\mathrm{i}}|n'_{\mathrm{i}}, J, K', \tau'_{\mathrm{inv}}\rangle$ are integrals over ρ; they are calculated numerically by means of Simpson's rule. Because of the symmetry, the functions integrated, $F(\rho)$ say, are always even or odd under the coordinate change $\rho \to \pi - \rho$ caused by the inversion operation E^*. Consequently we have

$$\int_0^{\pi} F(\rho)\,\mathrm{d}\rho = \begin{cases} 2\int_{\pi/2}^{\pi} F(\rho)\,\mathrm{d}\rho, & F(\rho)\ \text{even}, \\ 0, & F(\rho)\ \text{odd}, \end{cases} \qquad (93)$$

so that we only have to integrate the non-vanishing integrals over the interval $[\pi/2, \pi]$, i.e. the upper half of the definition interval $[0, \pi]$.

Matrix elements $\langle n''_{\mathrm{b}}, l''_{\mathrm{b}}, \tau''_{\mathrm{bend}}|\widehat{O}^{(p)}_{\mathrm{b}}|n'_{\mathrm{b}}, l'_{\mathrm{b}}, \tau'_{\mathrm{bend}}\rangle$ involving $(S^{\ell}_{4a}, S^{\ell}_{4b})$, p^{ℓ}_{4a}, and p^{ℓ}_{4b} are obtained from Nielsen [43]. The matrix elements for their products can be obtained numerically by the recursive procedure:

$$\langle nl|\xi^{\ell}_j F(\xi^{\ell}_n)|n'l'\rangle = \sum_{n''l''}\langle nl|\xi^{\ell}_j|n''l''\rangle\langle n''l''|F(\xi^{\ell}_n)|n'l'\rangle, \qquad (94)$$

$$\langle nl|p^{\ell}_j F(\xi^{\ell}_n)|n'l'\rangle = \sum_{n''l''}\langle nl|p^{\ell}_j|n''l''\rangle\langle n''l''|F(\xi^{\ell}_n)|n'l'\rangle. \qquad (95)$$

We have used Efremov's approach [46] to derive recursive numerical routines generating the one-dimensional integrals $\langle n+j|y^{\mu}|n\rangle$, $\langle n+j|y^{\mu}\,\mathrm{d}/\mathrm{d}r|n\rangle$, and $\langle n+j|y^{\mu}\,\mathrm{d}^2/\mathrm{d}r^2|n\rangle$ involving Morse-oscillator eigenfunctions and the Morse variable y. The stretching integrals $\langle n''_1|\langle n''_2|\langle n''_3|\widehat{O}^{(p)}_{\mathrm{s}}|n'_1\rangle|n'_2\rangle|n'_3\rangle$ are obtained from the one-dimensional integrals in a straightforward manner.

In the calculations presented in the following section, the basis set was truncated according to

$$2(n_1 + n_2 + n_3) + n_{\mathrm{b}} + n_{\mathrm{i}} \le 14 \qquad (96)$$

These limits correspond to the following matrix dimensions: $N_{A_1} = 1455$, $N_{A_2} = 1125$, $N_E = 2571$. With this basis set, we obtain convergence to about $0.5\,\mathrm{cm}^{-1}$ for energy values below $6100\,\mathrm{cm}^{-1}$. The ρ_k numerical grid, used to represent ρ-dependent functions, contained $N_{\mathrm{inv}} = 1000$ points.

In the variational calculations we employed sixth order expansions in the ξ^{ℓ}_n variables both for the kinetic energy part ($G_{\lambda,\mu}$ and U) and for the potential energy function (Type B). Although in our current realization of the recursive procedure in equation (50), the

expansions in equations (46, 47) can be taken up to eighth order, truncation after the sixth-order terms turned out to be sufficient in the present case; it produces convergence to about $0.02\,cm^{-1}$ for the vibrational energy values below $6100\,cm^{-1}$.

9. Calculations

We report here three sets of results obtained for $^{14}NH_3$ with the theoretical model described above: $J=0$ vibrational energies up to $6100\,cm^{-1}$, $J \leqslant 2$ energies for the vibrational ground state and the ν_2, ν_4, and $2\nu_2$ excited vibrational states, and $J \leqslant 7$ energies for the $4\nu_2^+$ vibrational state. The calculated energies are labeled by the quantum numbers of the basis state with the largest contribution to the eigenstate.

The calculations are based on an accurate *ab initio* potential energy surface, which is denoted as CBS**−45 760 [18] and may be viewed as an extension of our published CBS* surface [1]. Briefly, a regular grid with 45760 points was constructed that covered geometries with $0.85\,Å \leq r_1 \leq r_2 \leq r_3 \leq 1.20\,Å$ and $80^\circ \leq \alpha_{12},\ \alpha_{23},\ \alpha_{31} \leq 120^\circ$. Energies (ATZfc) were computed at all grid points using the CCSD(T) method (coupled cluster theory with all single and double substitutions [47] and a perturbative treatment of connected triple excitations [48, 49]) with the augmented correlation-consistent triple-zeta basis aug-cc-pVTZ [50, 51]. At 1460 selected points, more accurate energies (CBS+) were determined by extrapolating the CCSD(T) results to the complete basis set limit and including corrections for relativistic effects and core-valence correlation [1]. The differences between the ATZfc and CBS+ energies were fitted by a quintic polynomial in geometrically defined, internal coordinates, and the corrections were added to the ATZfc energies at all 45 760 grid points to generate the CBS**-45760 surface (which is close to CBS+ quality). An analytical representation of this surface was obtained by fitting a fifth-order expansion (57), through all CBS**-45760 data points. The resulting 130 potential parameters will be given elsewhere [18] and are also available from the authors on request.

In table 3, we compare calculated vibrational ($J=0$) term values with available, experimentally derived values and with theoretical results [3] for the 33 lowest vibrational levels (up to $6100\,cm^{-1}$). The root-mean-square (rms) deviation between the theoretical and experimental values is $4.7\,cm^{-1}$ in our case and $7.6\,cm^{-1}$ in the case of Colwell *et al.* [3].

Table 4 presents a comparison of our theoretical values of the $J=1$ and 2 energies in the vibrational ground state and the ν_2, ν_4, and $2\nu_2$ excited vibrational states with experimentally derived values [52, 53] and the theoretical results of Colwell *et al.* [3]. Here the rms deviations between theory and experiment, calculated for the 44 states listed in table 4, are $1.2\,cm^{-1}$ for our calculated energies and $6.0\,cm^{-1}$ for those of Colwell *et al.* [3]. For the vibrational ground state our theoretical term values are consistently slightly above the experimentally derived values, whereas those from [3] are significantly above the experimental values for high K and below them for low K, and thus show a less uniform behaviour. The largest contribution to the errors in the computed rovibrational term values comes from the vibrational term values. Adjusting the values of the ν_2, ν_4, and $2\nu_2$ band centres to coincide with experiment, our rms deviation for the rovibrational levels drops to $0.07\,cm^{-1}$, compared with $1.47\,cm^{-1}$ in the case of Colwell *et al.* [3].

In a recent experimental study of the $2\nu_4/\nu_1/\nu_3$ vibrational band system of $^{14}NH_3$, Kleiner *et al.* [28] observed weak absorption transitions to 23 rotational levels of a vibrational state which they assigned as the $(v_1, v_2^p, v_3^{l_3}, v_4^{l_4}) = (0, 4^+, 0^0, 0^0)$ state. A complete analysis of these transitions was not possible because of strong resonances not included in the model used for analysis [28]. We can now check the proposed assignment [28] by calculating theoretically the rotational structure in the $v_2^p = 4^+$ state up to $J=7$ (i.e. the highest rotational levels involved in the $4\nu_2^+$ transitions assigned). Such variational calculations for high J values are taxing: for example, in the case of $J=7$, we have to handle matrices of dimension 38 610 for E symmetry. This was not feasible with the available computational resources, and so we reduced the basis set to

$$n_i \leq 8, \quad 2(n_1 + n_2 + n_3) + n_b \leq 8,$$

which leads to matrices of dimension 6516 (A_1', A_2''), 6714 (A_1'', A_2'), and 13230 (E', E''). The term values obtained for the $v_2^p = 4^+$ state are listed in table 5, relative to the calculated zero point energy of $7446.279\,cm^{-1}$. To better appreciate the consistence, within the vibrational state, of the calculated rotational structure, the calculated energies for $J > 0$ are shifted by the deviation found for the $v_2^p = 4^+$, $J = 1$, $K = 0$ term value ($5.825\,cm^{-1}$). Table 5 also contains the experimentally derived term values taken from table 10 of [28].

The calculated energies are mostly in good agreement with the experimentally derived values, with one striking exception: The experimental term value of $3730.442\,cm^{-1}$, assigned to $(J, K, \Gamma) = (5, 1, E'')$, differs by $7.538\,cm^{-1}$ from the theoretical value. It has been obtained [28] as the upper level of two observed transitions, starting in levels with $(v_1, v_2^p, v_3^{l_3}, v_4^{l_4}, J, K, \Gamma) = (0, 0^-, 0^0, 0^0, 6, 1, E')$ [$3317.204\,cm^{-1}$] and

Table 3. Vibrational term values[a] for $^{14}NH_3$ (in cm^{-1}).

Γ	$v_1 v_2^p v_3^{l_3} v_4^{l_4}$	Obs.[b]	Calc.	Obs.-Calc.	Ref. [3][c]
A'	$01^+0^00^0$	932.43	933.75	−1.32	942.88
A'	$02^+0^00^0$	1597.47	1598.67	−1.20	1613.10
A'	$03^+0^00^0$	2384.15	2387.66	−3.51	2382.66
A'	$00^+0^02^0$	3216.02	3213.77	2.25	3215.08
A'	$10^+0^00^0$	3336.02	3341.58	−5.56	3321.26
A'	$04^+0^00^0$	3462.00	3468.35	−6.35	3456.59
A'	$01^+0^02^0$	4115.62	4099.92	15.70	4124.44
A'	$11^+0^00^0$	4294.51	4301.40	−6.89	4289.83
E'	$00^+0^01^1$	1626.28	1626.00	0.28	1626.79
E'	$01^+0^01^1$	2540.53	2537.13	3.40	2549.78
E'	$00^+0^02^2$	3240.18	3238.62	1.56	3240.97
E'	$00^+1^10^0$	3443.68	3446.23	−2.55	3440.79
E'	$01^+1^10^0$	4416.91	4420.95	−4.04	4426.04
E'	$10^+0^01^1$	4955.85	4960.23	−4.38	4941.33
E'	$00^+1^11^1$	5052.60	5054.77	−2.17	5054.32
E'	$01^+1^11^1$	6012.90	6012.59	0.31	6023.87
A''	$00^-0^00^0$	0.79	0.80	−0.01	0.60
A''	$01^-0^00^0$	968.12	969.80	−1.68	973.30
A''	$02^-0^00^0$	1882.18	1885.04	−2.86	1883.57
A''	$03^-0^00^0$	2895.51	2900.27	−4.76	2889.79
A''	$00^-0^02^0$	3217.59	3215.61	1.98	3216.69
A''	$10^-0^00^0$	3337.08	3342.62	−5.54	3322.76
A''	$04^-0^00^0$	4055.00[d]	4068.65	−13.65[d]	4054.53
A''	$01^-0^02^0$	4173.25	4164.34	8.91	4175.72
A''	$11^-0^00^0$	4320.06	4327.16	−7.10	4313.71
E''	$00^-0^01^1$	1627.37	1627.16	0.21	1627.64
E''	$01^-0^01^1$	2586.13	2584.75	1.38	2589.20[e]
E''	$00^-0^02^2$	3241.61	3240.17	1.44	3242.03
E''	$00^-1^10^0$	3443.99	3446.60	−2.61	3441.07
E''	$01^-1^10^0$	4435.4	4439.69	−4.29	4441.49
E''	$10^-0^01^1$	4956.79	4961.51	−4.72	4942.76
E''	$00^-1^11^1$	5052.97	5055.41	−2.44	5054.77
E''	$01^-1^11^1$	6037.12	6037.40	−0.28	6043.99
rms				4.7	

[a]Labeled by $(v_1, v_2^p, v_3^{l_3}, v_4^{l_4})$, where the v_r and l_r are usual harmonic oscillator quantum numbers and $p = +(-)$ indicates the lower, symmetric (upper, antisymmetric) inversion component.
[b]Experimentally derived values taken from [1], which also contains the references to the experimental work.
[c]Theoretical values from Colwell *et al.* [3], Table 7.
[d]The original experimental value [55] for the $4\nu_2^g$ band centre is $4055 \pm 5\,cm^{-1}$. A misprinted value of $4045\,cm^{-1}$ appeared later [56] and was used in many compilations. We use the original value [55] but do not include it when calculating rms deviations because of its high uncertainty.
[e]Originally [3] given as $1589.20\,cm^{-1}$. We have corrected this obvious misprint and use $2589.20\,cm^{-1}$, which is also consistent with the quoted inversion splitting [3].

$(0, 0^-, 0^0, 0^0, 4, 1, E')$ [$3534.830\,cm^{-1}$], respectively, where the respective observed wavenumbers are given in square brackets. However, Appendix 1 of [28] also lists two transitions with wavenumbers at 3317.20623 and $3534.83109\,cm^{-1}$, that are assigned to the ν_1 and ν_3 bands, respectively. The wavenumbers of these transitions are very close (within $0.002\,cm^{-1}$) to those of the two transitions assigned to end in the level at $3730.442\,cm^{-1}$. Apparently, the proposed assignment [28] assumes that two weak transitions to the $4\nu_2^+(J, K, \Gamma) = (5, 1, E'')$ level are hidden under the relatively strong lines at $3317.20623\,cm^{-1}(\nu_1)$ and $3534.83109\,cm^{-1}(\nu_3)$, respectively, whereas our calculations predict these $4\nu_2$ transitions to be shifted about $7.5\,cm^{-1}$ away from the positions of these lines.

Closer inspection of table 5 shows that there are two further rovibrational levels with smaller, but rather unsystematic deviations from the experimentally derived term values [28]: $(J, K, \Gamma) = (5, 2, E'')$ predicted at $3715.255\,cm^{-1}$ (obs−calc is $-0.987\,cm^{-1}$), and

Table 4. Rotation–vibration term values[a] of $^{14}NH_3$ for $J = 1$ and 2 (in cm^{-1}).

v_1	v_2^p	$v_3^{l_3}$	$v_4^{l_4}$	Γ	J	K	Obs.[b]	Calc.	Obs.-Calc	Ref. [3][c]
0	0^+	0^0	0^0	E''	1	1	16.13	16.22	−0.09	16.27
				A_2'	1	0	19.89	19.91	−0.02	19.71
				E'	2	2	44.84	44.85	−0.01	45.37
				E''	2	1	55.91	56.00	−0.09	55.69
				A_1'	2	0	59.60	59.73	−0.13	59.10
0	0^-	0^0	0^0	E'	1	1	16.93	16.99	−0.06	16.87
				A_1''	1	0	20.67	20.70	−0.03	20.31
				E''	2	2	45.51	45.64	−0.13	45.97
				E'	2	1	56.67	56.78	−0.11	56.27
				A_2''	2	0	60.39	60.49	−0.10	59.68
0	1^+	0^0	0^0	E''	1	1	948.57	949.93	−1.36	959.10
				A_2'	1	0	952.56	953.92	−1.36	962.85
				E'	2	2	976.78	978.29	−1.51	987.84
				E''	2	1	988.81	990.24	−1.43	990.04
				A_1'	2	0	992.82	994.24	−1.42	1002.78
0	1^-	0^0	0^0	E'	1	1	984.13	985.86	−1.73	989.44
				A_1''	1	0	987.86	989.60	−1.74	993.05
				E''	2	2	1012.43	1014.25	−1.82	1018.30
				E'	2	1	1023.67	1025.45	−1.78	1028.85
				A_2''	2	0	1027.42	1029.18	−1.76	1032.53
0	0^+	0^0	1^1	E''	1	1	1639.47	1639.34	0.13	1640.14
				A_2''	1	1	1645.39	1645.11	0.28	1646.11
				E'	1	0	1646.59	1646.40	0.19	1647.01
				A_2'	2	2	1664.97	1665.00	−0.03	1666.23
				E'	2	2	1677.27	1677.10	0.17	1678.49
				E''	2	1	1680.17	1680.09	0.08	1680.61
				A_2''	2	1	1687.24	1687.08	0.16	1687.39
				E'	2	0	1687.33	1687.20	0.13	1687.46
0	0^-	0^0	1^1	E'	1	1	1640.45	1640.47	−0.02	1640.97
				A_2'	1	1	1647.30	1647.11	0.19	1647.89
				E''	1	0	1647.79	1647.63	0.16	1648.04
				A_2''	2	2	1665.98	1666.12	−0.14	1667.03
				E''	2	2	1678.61	1678.43	0.18	1679.79
				E'	2	1	1681.36	1681.36	0.00	1681.66
				A_2'	2	1	1686.54	1686.40	0.14	1686.89
				E''	2	0	1688.71	1688.65	0.06	1688.96
0	2^+	0^0	0^0	E''	1	1	1613.57	1614.82	−1.25	1629.20
				A_2'	1	0	1617.84	1619.06	−1.22	1633.18
				E'	2	2	1641.52	1642.88	−1.36	1657.54
				E''	2	1	1654.29	1655.56	−1.27	1669.33
0	2^-	0^0	0^0	E'	1	1	1898.02	1900.90	−2.88	1899.55
				E''	2	2	1926.12	1929.13	−3.01	1928.36
				E'	2	1	1936.87	1939.69	−2.82	1938.44
				A_2''	2	0	1940.29	1943.22	−2.93	1942.22

[a]Labeled by $(v_1, v_2^p, v_3^{l_3}, v_4^{l_4})$, where the v_r and l_r are usual harmonic oscillator quantum numbers and $p = +(-)$ indicates the lower, symmetric (upper, antisymmetric) inversion component.
[b]Experimentally derived values from [52] and [53].
[c]Theoretical values from Colwell *et al.* [3].

$(J, K, \Gamma) = (5, 5, E'')$ predicted at $3665.142\,cm^{-1}$ (obs−calc is $-2.206\,cm^{-1}$).

For the remaining 20 rotational term values in table 5, our calculations confirm the suggested assignments [28] because the deviations between experimentally derived and computed values are small ($0.35\,cm^{-1}$ or less) and systematic. In the other three cases (see above) the original assignment should be reconsidered, especially for $4\nu_2^+$ $(5, 1, E'')$, where the deviation of $7.5\,cm^{-1}$ is exceedingly large. It should

Table 5. Rotational term values for the $4\nu_2^+$ vibrational state of $^{14}NH_3$ (in cm^{-1}).

J	K	Γ	Obs.[a]	Calc.-5.825	Obs.-Calc.
1	0	A_2'	3479.614	3479.614	0.000
1	1	E''	3477.113	3477.460	−0.347
2	2	E'	3505.184	3505.237	−0.053
2	1	E''	3511.913	3511.865	0.048
3	0	A_2'	3566.580	3566.508	0.072
3	2	E'	3557.040	3556.978	0.062
3	3	A_1''	3545.710	3545.795	−0.085
3	3	A_2''	3545.710	3545.795	−0.085
3	1	E''	3564.175	3564.100	0.075
4	4	E'	3598.973	3599.106	−0.133
4	2	E'	3627.017	3626.970	0.047
4	3	A_1''	3614.926	3614.861	0.065
4	3	A_2''	3614.927	3614.860	0.067
4	1	E''	3634.403	3634.402	0.001
5	4	E'	3685.472	3685.398	0.074
5	2	E'	3714.268	3715.255	−0.987
5	3	A_1''	3702.653	3702.650	0.003
5	3	A_2''	3702.653	3702.652	0.001
5	5	E''	3662.936	3665.142	−2.206
5	1	E''	3730.442	3722.904	7.538
6	6	A_1'	3743.604	3743.879	−0.275
6	6	A_2'	3743.604	3743.879	−0.275
6	4	E'	3790.983	3791.033	−0.050
6	3	A_1''	3808.781	3808.931	−0.150
6	3	A_2''	3808.781	3808.927	−0.146
6	5	E''	3768.609	3768.508	0.101
6	1	E''	3829.337	3829.565	−0.228
7	6	A_1'	3864.252	3864.080	0.169

[a]Experimentally derived values from [28].

be noted that a later experimental investigation of the $4\nu_2-\nu_2$ hot band [54] confirmed most of the original assignments [28] but did not address the three critical cases discussed above.

10. Summary and conclusion

In the preceding sections we have presented, in considerable detail, a new variational model for describing the rotation–vibration motion of pyramidal XY_3 molecules, which is based on the Hougen-Bunker-Johns approach [5]. We introduce a flexible reference configuration that follows the large-amplitude vibration (i.e. the inversion motion in NH_3) and the remaining small-amplitude vibrations are described as displacements from this configuration. In this way, we obtain a model with maximum separation between the different types of molecular motion. The price paid for this advantage is that we need to approximate the kinetic energy operator by a finite power-series expansion in the small-amplitude vibrational parameters.

We report three applications, all for $^{14}NH_3$, of the model developed addressing the $J=0$ vibrational energies to high excitation, the $J \leqslant 2$ energies for the vibrational ground state and the ν_2, ν_4, and $2\nu_2$ excited vibrational states, and the $J \leqslant 7$ energies for the $4\nu_2^+$ vibrational state. The calculations are based on the CBS**-45760 potential energy surface described elsewhere [1, 18].

We have compared our calculated energies to experimental data and to recent theoretical results by Colwell *et al.* [3]. We achieve very satisfactory agreement with experiment for both the purely vibrational term

values and the rotational spacings. This demonstrates the high accuracy of the CBS**-45760 potential energy surface and the soundness of our approach to the solution of the rotation–vibration problem.

Our theoretical calculation largely verifies the tentative assignments made by Kleiner *et al.* [28] of transitions in the $4\nu_2^+$ band of $^{14}NH_3$. The proposed quantum number labels for 23 experimentally derived, rotational term values in the $v_2^p = 4^+$ *v*ibrational state are confirmed in 20 cases, and theoretical predictions are made for the remaining three cases, particularly for $4\nu_2$ $(5, 1, E'')$ where a misassignment is most likely.

This last example shows that theoretical calculations of rotation–vibration energies can now be carried out also for four-atomic molecules with sufficient accuracy to be helpful in the interpretation and assignment of experimental, high-resolution rotation–vibration spectra. It also demonstrates that our approach can be applied to rotation–vibration states with higher J values (here up to $J = 7$) where exact variational treatments of nuclear motion are no longer feasible. This advantage arises from the maximum separation of different types of motion that is inherently built into our approach.

Acknowledgements

This work was supported by the European Commission through contract no. HPRN-CT-2000-00022 'Spectroscopy of Highly Excited Rovibrational States'. S. Yu. acknowledges financial support from NSERC (Canada) and thanks P. Bunker and S. Patchkovskii for helpful discussions.

References

[1] H. Lin, W. Thiel, S.N. Yurchenko, M. Carvajal, P. Jensen, *J. Chem. Phys.*, **117,** 11265–11276 (2002).
[2] S.N. Yurchenko, M. Carvajal, P. Jensen, F. Herregodts, T.R. Huet, *Chem. Phys.*, **290,** 59–67 (2003).
[3] S.M. Colwell, S. Carter, N.C. Handy, *Mol. Phys.*, **101,** 523–544 (2003).
[4] C. Léonard, N.C. Handy, S. Carter, J.M. Bowman, *Spectrochim. Acta A*, **58,** 825–838 (2002).
[5] J.T. Hougen, P.R. Bunker, J.W.C. Johns, *J. Mol. Spectrosc.*, **34,** 136-172 (1970).
[6] D. Papoušek, J.M.R. Stone, V. Špirko, *J. Mol. Spectrosc.*, **48,** 17–37 (1973).
[7] V. Špirko, *J. Mol. Spectrosc.*, **101,** 30–47 (1983).
[8] D. Papoušek, M.R. Aliev, *Molecular Vibrational-Rotational Spectra*, Elsevier, Amsterdam (1982).
[9] A.R. Hoy, P.R. Bunker, *J. Mol. Spectrosc.*, **52,** 439–456 (1974).
[10] A.R. Hoy, P.R. Bunker, *J. Mol. Spectrosc.*, **74,** 1–8 (1979).
[11] P. Jensen, *Comp. Phys. Rep.*, **1,** 1–55 (1983).
[12] P. Jensen, *J. Mol. Spectrosc.*, **128,** 478–501 (1988).
[13] P. Jensen, *Mol. Phys.*, **98,** 1253–1285 (2000).
[14] S.V. Shirin, O.L. Polyansky, N.F. Zobov, P. Barletta, J. Tennyson, *J. Chem. Phys.*, **118,** 2124–2129 (2003).
[15] O.L. Polyansky, A. G. Császár, S.V. Shirin, N.F. Zobov, P. Barletta, J. Tennyson, D.W. Schwenke, P.J. Knowles, *Science*, **299,** 539–542 (2003).
[16] T. Rajamäki, A. Miani, L. Halonen, *J. Chem. Phys.*, **118,** 6358–6369 (2003).
[17] T. Rajamäki, A. Miani, L. Halonen, *J. Chem. Phys.*, **118,** 10929–10938 (2003).
[18] H. Lin, J.J. Zheng, S.N. Yurchenko, P. Jensen, W. Thiel, to be published.
[19] E. Kauppi, L. Halonen, *J. Chem. Phys.*, **103,** 6861–6872 (1995).
[20] F. Gatti, *J. Chem. Phys.*, **111,** 7225–7235 (1999).
[21] F. Gatti, C. Iung, C. Leforestier, X. Chapuisat, *J. Chem. Phys.*, **111,** 7236–7243 (1999).
[22] N.C. Handy, S. Carter, S.M. Colwell, *Mol. Phys.*, **96,** 477–491 (1999).
[23] D. Luckhaus, *J. Chem. Phys.*, **113,** 1329–1347 (2000).
[24] J. Pesonen, A. Miani, L. Halonen, *J. Chem. Phys.*, **115,** 1243–1250 (2001).
[25] T. Rajamäki, A. Miani, J. Pesonen, L. Halonen, *Chem. Phys. Lett.*, **363,** 226–232 (2002).
[26] C. Léonard, S. Carter, N.C. Handy, *Chem. Phys. Lett.*, **370,** 360–365 (2003).
[27] H.-G. Yu, T. Muckerman, *J. Molec. Spectrosc.*, **214,** 11–20 (2002).
[28] I. Kleiner, L.R. Brown, G. Tarrago, Q.-L. Kou, N. Picqué, G. Guelachvili, V. Dana, J.-Y. Mandin, *J. Mol. Spectrosc.*, **193,** 46–71 (1999).
[29] A.G. Császár, W.D. Allen, H.F. Schaefer, *J. Chem. Phys.*, **108,** 9751–9764 (1998).
[30] W. Klopper, C.C.M. Samson, G. Tarczay, A.G. Császár, *J. Comput. Chem.*, **22,** 1306–1314 (2001).
[31] P.R. Bunker, P. Jensen, *Molecular Symmetry and Spectroscopy*, 2nd ed., NRC Research Press, Ottawa (1998).
[32] P. Schwerdtfeger, L.J. Laakkonen, P. Pyykkö, *J. Chem. Phys.*, **96,** 6807–6819 (1992).
[33] G.O. Sørensen, *Topics in Current Chemistry*, M.J.S. Dewar *et al.* (Eds.), Vol. 82, p. 97–175. Springer-Verlag, Heidelberg (1979).
[34] A. Nauts, X. Chapuisat, *Mol. Phys.*, **55,** 1287–1318 (1985).
[35] B. Podolsky, *Phys. Rev.*, **32,** 812–816 (1928).
[36] C. Eckart, *Phys. Rev.*, **47,** 552–558 (1935).
[37] A. Sayvetz, *J. Chem. Phys.*, **7,** 383–389 (1939).
[38] A.R. Hoy, I.M. Mills, G. Strey, *Mol. Phys.*, **24,** 1265–1290 (1972).
[39] E.B. Wilson Jr, J.C. Decius, P.C. Cross, *Molecular Vibrations*, Dover Publications, Inc., New York (1995).
[40] V. Špirko, P. Jensen, P.R. Bunker, A. Čejchan, *J. Mol. Spectrosc.* **112,** 183–202 (1985).
[41] B. Numerov, *Publ. of the Central Astrophys. Observatory (Rus)*, **2,** 188–259 (1923).
[42] J.W. Cooley, *Math. Comp.*, **15,** 363–374 (1961).
[43] H.H. Nielsen, *Rev. Mod. Phys.*, **23,** 90–136 (1951).
[44] M. Abramowitz, I. Stegun, *Handbook of Mathematical Functions*, Dover Pub., New York (1972).

[45] P.M. Morse, *Phys. Rev.*, **34,** 57–64 (1929).
[46] Yu. S. Efremov, *Opt. Spectrosc.*, **43,** 693–694 (1977).
[47] G.D. Purvis, R.J. Bartlett, *J. Chem. Phys.*, **76,** 1910–1918 (1982).
[48] M. Urban, J. Noga, S.J. Cole, R.J. Bartlett, *J. Chem. Phys.*, **83,** 4041–4046 (1985).
[49] K. Raghavachari, G.W. Trucks, J.A. Pople, M. Head-Gordon, *Chem. Phys. Lett.*, **157,** 479–483 (1989).
[50] T.H. Dunning, *J. Chem. Phys.*, **90,** 1007–1023 (1989).
[51] D.E. Woon, T.H. Dunning, *J. Chem. Phys.*, **98,** 1358–1371 (1993).
[52] Š. Urban, V. Špirko, D. Papoušek, J. Kauppinen, S.P. Belov, L.I. Gershtein, A.F. Krupnov, *J. Mol. Spectrosc.*, **88,** 274–292 (1981).
[53] J.S. Garing, H.H. Nielsen, K. Narahari Rao, *J. Mol. Spectrosc.*, **3,** 496–527 (1959).
[54] C. Cottaz, G. Tarrago, I. Kleiner, L.R. Brown, *J. Mol. Spectrosc.*, **209,** 30–49 (2001).
[55] L.D. Ziegler, B. Hudson, *J. Phys. Chem.*, **88,** 1110–1116 (1984).
[56] P. Rosmus, P. Botschwina, H.-J. Werner, V. Vaida, P.C. Engelking, M.I. McCarthy, *J. Chem. Phys.*, **86,** 6677–6692 (1987).